Water Vapour in the Climate System - Summer School Cargese, 2009
Lecture notes Stephan Fueglistaler

S. Fueglistaler / T. Flannaghan
DAMTP, U. Cambridge

August 2009

Courses

16/09, Wednesday, Water vapour 4, The Tropical Tropopause Layer

22/09, Tuesday, Water vapour 9

23/09, Wednesday, Water vapour 10, 12

About this document

This document is a compilation of material for the WAVACS summer school, Cargese 2009. As such, it's scope is limited; and please let me know if you find errors of any sort.

Contents

1 The Tropical Tropopause Layer

Lecture overview

In this section we will discuss the tropical tropopause layer from a phenomenological perspective; and will relate observed properties to theory.

Key aspects

Exchange between troposphere and stratosphere may occur through isentropic or diabatic transport; transport into the stratospheric overworld occurs diabatically across the TTL, and conditions therein regulate to some extent (depending on tracer; prominent examples are water vapour, and so-called Very Short Lived Substances) the flux of tracers into the stratosphere.

The concept of a tropopause layer - in contrast to the traditional tropopause - reflects the fact that many observables like temperature and winds, trace gas concentrations, and processes, exhibit in one way or another dual characteristics in a transition layer. A number of definitions have been put forward which - inevitably for a 'transition' layer - differ somewhat, and reflect different motivations and interests of the authors.

Here, I will introduce the TTL along the lines of the Fueglistaler *et al.*, 2009.Rev. Geophysics article, this is by no means the only possible perspective on the TTL (see discussion in aforementioned article), and interested readers are encouraged to study the bibliography to learn about other approaches.

While it can be argued that any subdivions in a geophysical fluid bears an element of arbitrariness (and even more so for a transition between two 'pure' layers), a number of factors certainly allow to make a case for a tropical tropopause layer.

The basic distinction troposphere/stratosphere from a dynamical point of view (as opposed to simply studying the thermal structure) is based on:

- The tropical tropospheric circulation is a thermally direct circulation, that is, the latitudinal gradient in net gain of energy from irradiation leads to a dynamically unstable situation; in the tropics (small Coriolis force) convection plays the key role (i.e. latent heat release balances radiative loss to space; plus export to higher latitudes).

- In the stratosphere, the circulation is what is called 'wave driven', that is, the latitudinal gradient in absorbed radiation (downwelling as well as upwelling) implies a temperature gradient which, however, in principle can be balanced by the Coriolis force (we note the possibility of a direct 'Hadley-type' circulation, which in practise is, however, much weaker and in fact masked, by the wave-driven circulation). The observed stratospheric circulation is due to momentum deposition of upward propagating

waves - the so-called Eliassen-Palm Flux divergence (see *Holton et al.,* 1995).

Most prominent *manifestations* of this mechanism are the Quasi-Biennial Oscillation (where the momentum deposition leads to acceleration due to the small Coriolis force; see *Baldwin et al.,* 2001), and the seasonal (and longer-term) variations in the strength of the B-D circulation.

In the TTL, these two very different types of circulations produce a rich mix of effects, which are, unfortunately, often difficult to attribute unambigously to one or the other process.

Moreover, a few processes and effects are very specific to the TTL.

- The thermal effect of convection may be opposite to the usual; convection penetrating the TTL may have to overshoot its level of neutral buoyancy (LNB, which is typically less than about 15km); and mixing of this overshoot with ambient air *cools* the environment (think of mixing of potential temperatures, where the potential temperature of the convective plume equals that of the ambient profile at the height of the LNB, and remains constant thereafter while the ambient pot. temperature still increases).

- The flow and temperatures are marked by very prominent quasi-stationary structures. They are usually explained in terms of the Matsuno-Gill pattern (but note original paper by Gill does *not* address the upper-level response to tropospheric heating patterns). These patterns are the result of the distribution of convection (heating) *below*, i.e in the troposphere proper.

The TTL: Gate for H_2O and VSLS

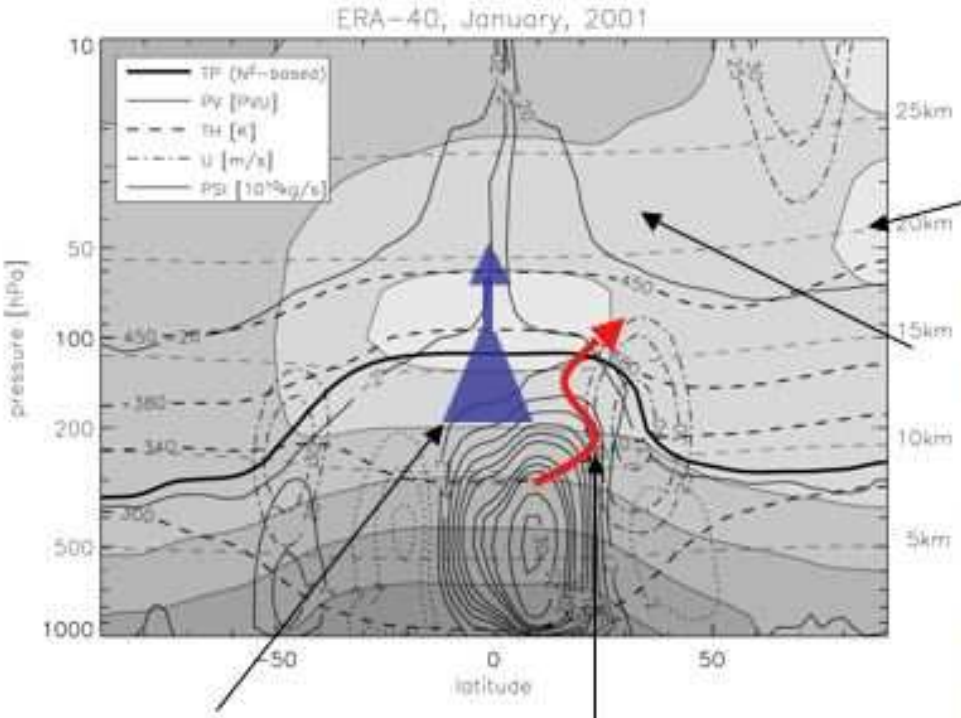

Chemistry:

H2O: Source of OH, het. chem. on PSCs.

VSLS: O3 depletion.

Radiation:

H_2O and O_3 trends -> rad. forcing, changes in strat. circulation with impact on tropospheric circulation (e.g. NAO).

Temperature "bottleneck" for stratospheric H_2O; **entry mixing ratio $[H_2O]_e$.**

Time "bottleneck" for **VSLS** (order weeks).

Figure 1:

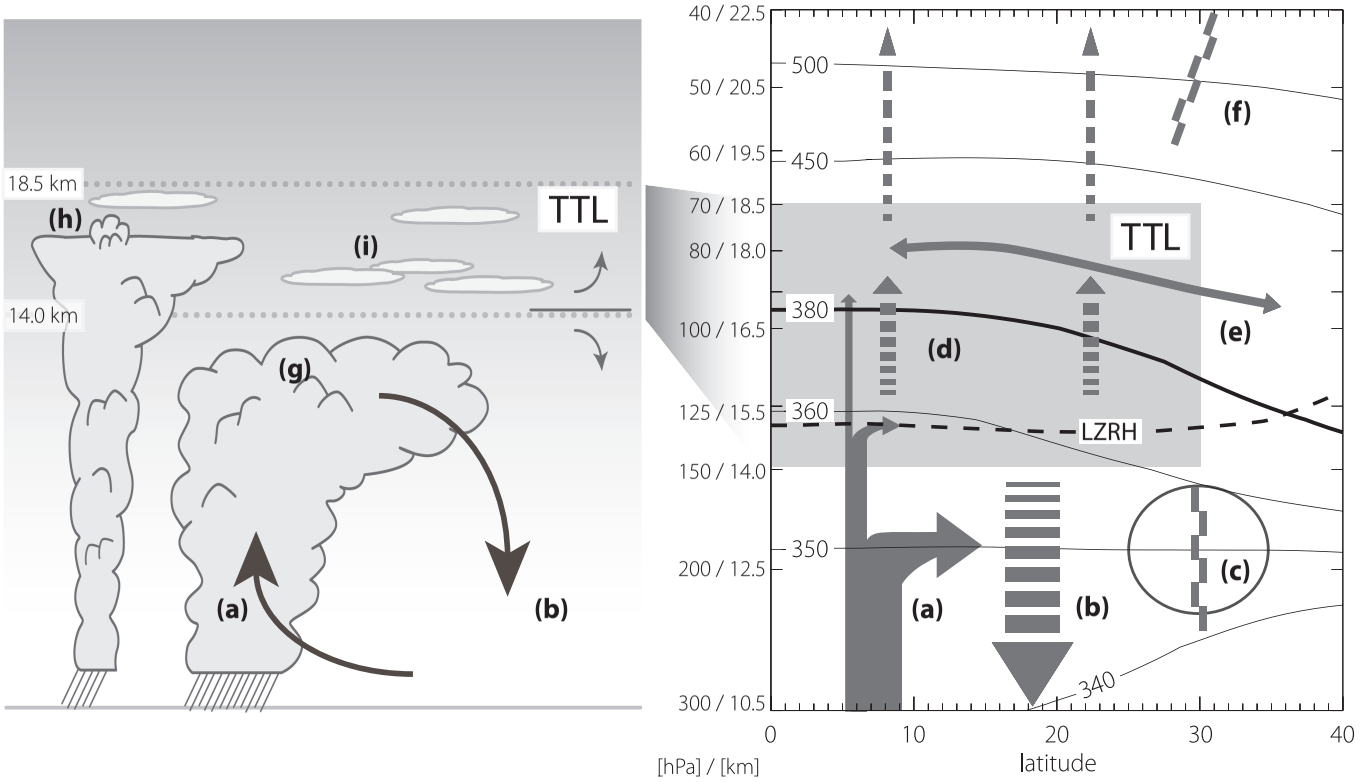

Figure 2: Schematic of cloud processes and transport (left) and of zonal mean circulation (right). Arrows indicate circulation, black dashed line is *clear sky* level of zero net radiative heating (LZRH), black solid lines show isentropes (in Kelvin; based on ERA-40). (a) Deep convection: Main outflow around 200 hPa, outflow rapidly decays with height in TTL, rare penetrations of tropopause. Fast vertical transport of tracers from boundary layer into the TTL. (b) Radiative cooling (subsidence). (c) Subtropical jets, limit quasi-isentropic exchange between troposphere and stratosphere (transport barrier). (d) Radiative heating, balances forced diabatic ascent. (e) Rapid meridional transport of tracers, mixing. (f) Edge of the 'tropical pipe', relative isolation of tropics and stirring over extratropics ('the surf zone'). (g) Deep convective cloud. (h) Convective core overshooting its level of neutral buoyancy. (i) Ubiquitous optically (and geometrically) thin, horizontally extensive cirrus clouds, often formed *insitu*. Note: The height-pressure-potential temperature relations shown are based on tropical annual mean temperature fields, with height values rounded to the nearest 0.5 km. Fueglistaler *et al.*, 2009.

1.1 Temperature

The tropical tropopause is one of the coldest places in Earth's atmosphere. In the tropical troposphere, the temperature profile follows closely that of a moist-adiabate. From about 200 hPa (12.5km) upwards, the static stability increases and reaches a local maximum just above the tropical tropopause. (In passing we note that the observed departure from a moist adiabatic lapse rate far below the tropopause renders a *direct* connection (i.e. through lapse-rate arguments, as sometimes found in the literature) between sea surface temperatures and tropopause temperatures irrelevant.)

Temperatures in the tropical lower stratosphere show a pronounced annual cycle, with a peak-to-peak amplitude of about 8 K at 70 hPa.

The variations over the subtropics are due to the seasonal shift in the position of the subtropical jets following the seasonal migration of the 'Hadley-cell'.

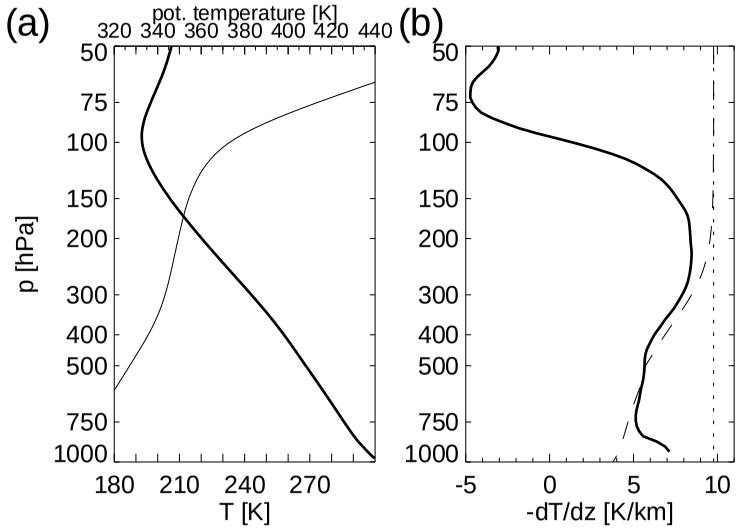

Figure 3: Temperature and lapse-rate, from Fueglistaler *et al.*, 2009..

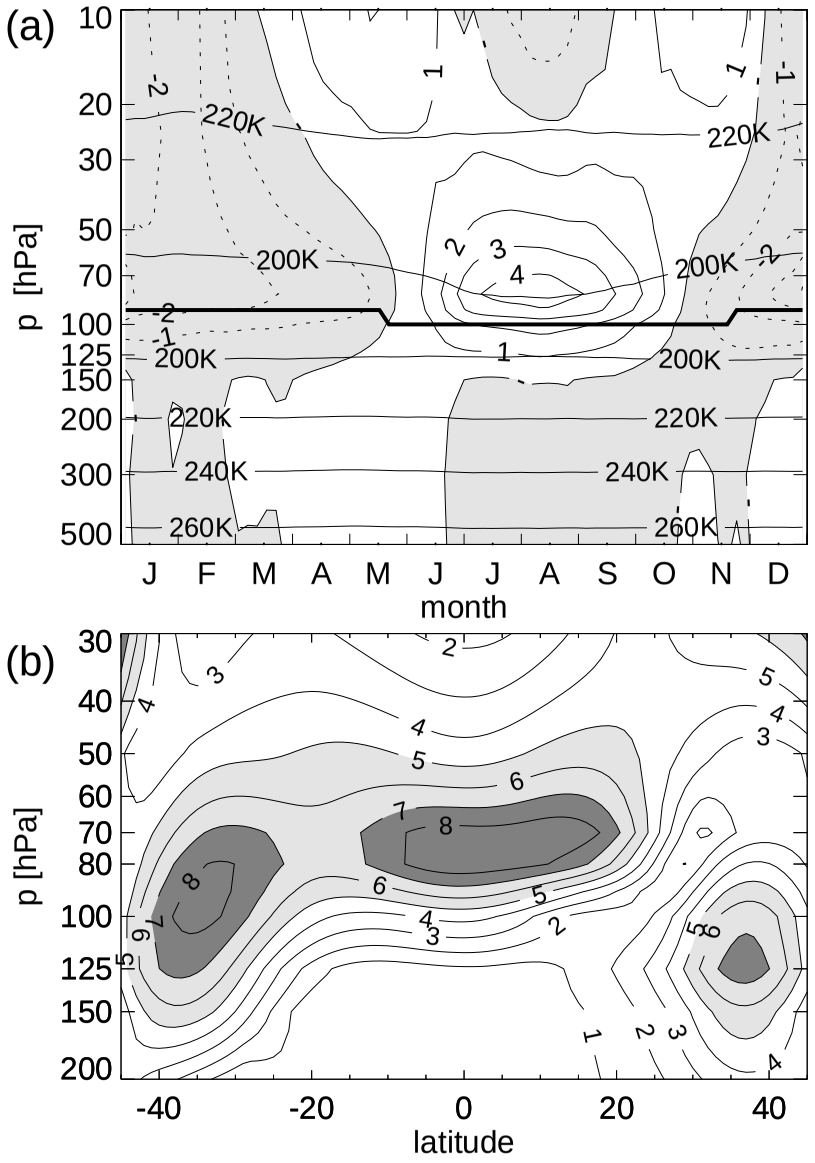

Figure 4: Annual cycle of temperatures, Fueglistaler *et al.*, 2009..

1.2 Zonal structure

Observation:

The tropics show a pronounced quasi-stationary structure in circulation and temperature (and, associated with the former, in various other trace gases).

The conventional description for the tropical tropospheric circulation is that of the 'Walker circulation'; with convective ascent focused over the Western Pacific area, and descent over the Eastern Pacific; see also the fundamental paper by Gill [1981]. (Note: a common mistake is to think the air rises steadily over the Western Pacific; instead, air is also radiatively subsiding in these regions, but the **local** convective mass flux exceeds the **local** radiative descent; with the net surplus balancing the net subsidence elsewhere.

Of particular interest is the quasi-stationary temperature structure in the TTL. (Responsible mechanism may be discussed offline.)

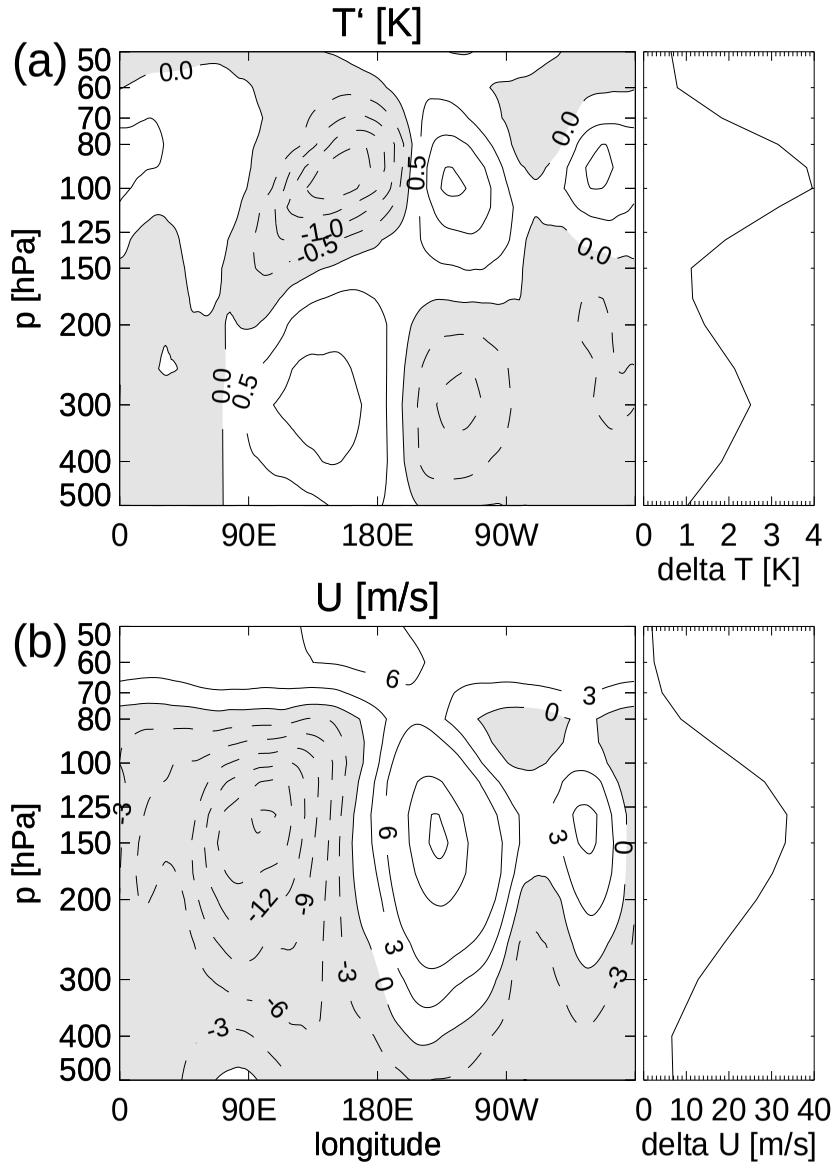

Figure 5: Temperature and zonal wind structure. Fueglistaler *et al.*, 2009.

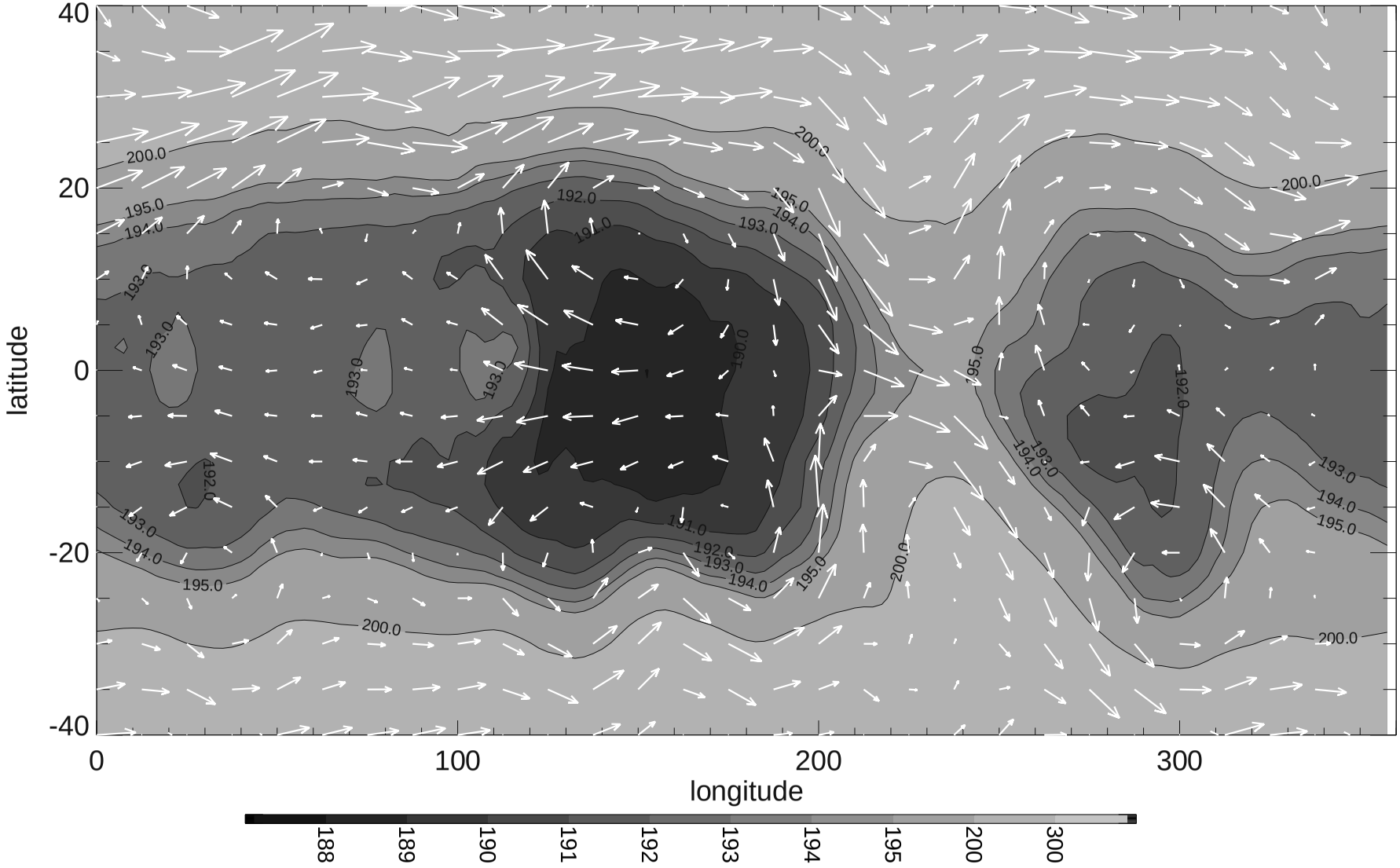

Figure 6: Temperature and wind map. Data: ERA-40, January 2000, 100hPa.

1.3 Ozone

Observation

Ozone begins to increase in the TTL; in the troposphere shows an 'S'-type profile, particularly over the Pacific. Maritime boundary layer has very low ozone concentrations; minimum at base of TTL explained in terms of detrainment from convection. Increase in mid-troposphere due to in-situ production, and (quasi-isentropic) inmixing from stratosphere (the authorative paper on this topic remains to be written).

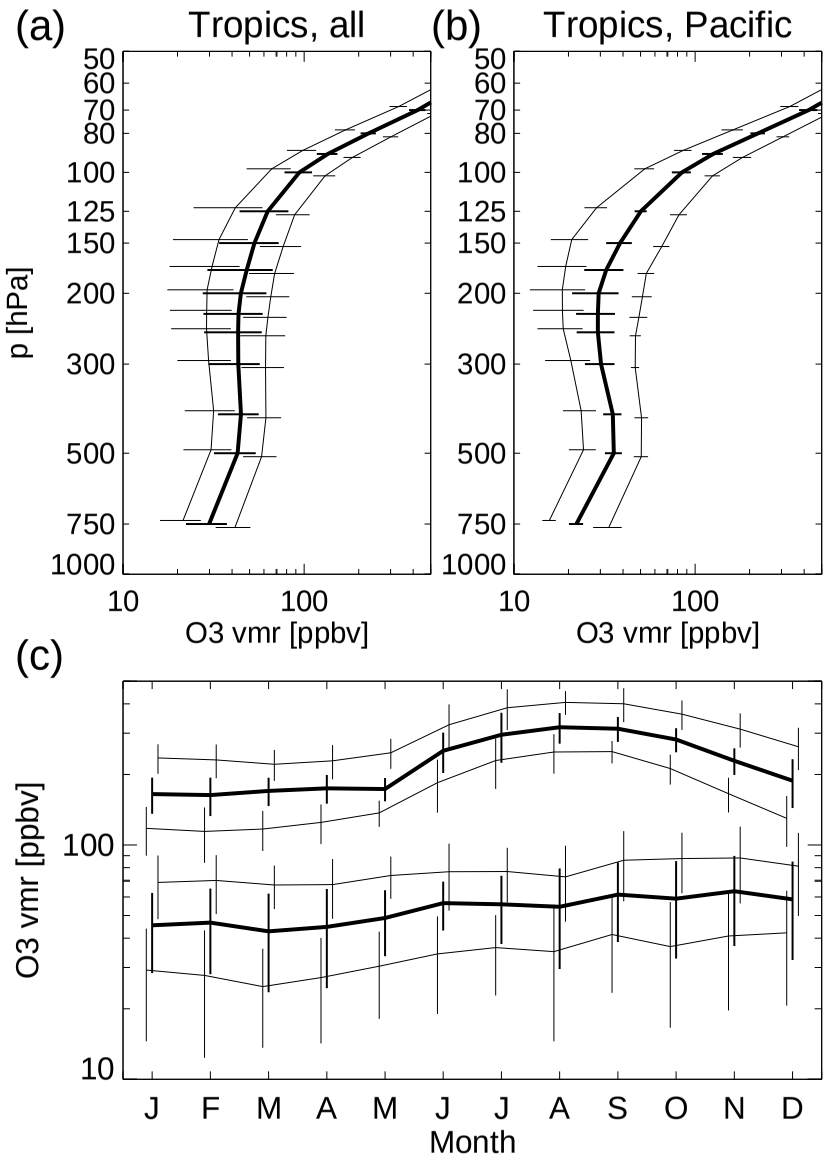

Figure 7: Ozone profiles, and annual cycle on 150 hPa and 80 hPa. Fueglistaler *et al.*, 2009.

1.4 Water vapour and isotopologues

Much of water vapour (and variability) in the TTL will be covered later, and elsewhere. Hence, we restrict ourselves here to a few basic aspects.

Observation:

First, we note that - as a consequence of the extremely low temperatures - the TTL is also exceptionally dry, with mixing ratios at the tropopause of sometimes as low as 1 ppmv (on average about 3-4ppmv). An ongoing issue is the accuracy of measurements at these low concentrations, and the problem that sufficient spatio-temporal coverage for a global perspective can be achieved with (space borne) remote sensing instruments only, which have, however, a coarse vertical resolution.

On the other hand, relative humidity is very high in the TTL - again, this is simle to understand: (a) It is the coldest place anyway (and hence has lowest saturation mixing ratio), (b) the general motion is upward, and hence an 'air parcel' experiences continous cooling up to the cold point tropopause (we will discuss important modifications of this aspect later on).

Because temperatures increase from the tropopause upward, the TTL controls how much water enters the stratosphere, with only little modifications thereafter in the stratosphere. A consequence of this, and the annual cycle of tropopause temperatures, is the so-called 'atmospheric tape recorder' (*Mote et al.*, 1995; *Weinstock et al.* 1995).

Water isotopologues such as HDO show an interesting behaviour, in that they depart from a so-called 'Rayleigh curve' (explained elsewhere; the basic equation is $dln[\mathrm{HDO}] = \alpha(T) dln[\mathrm{H2O}]$).

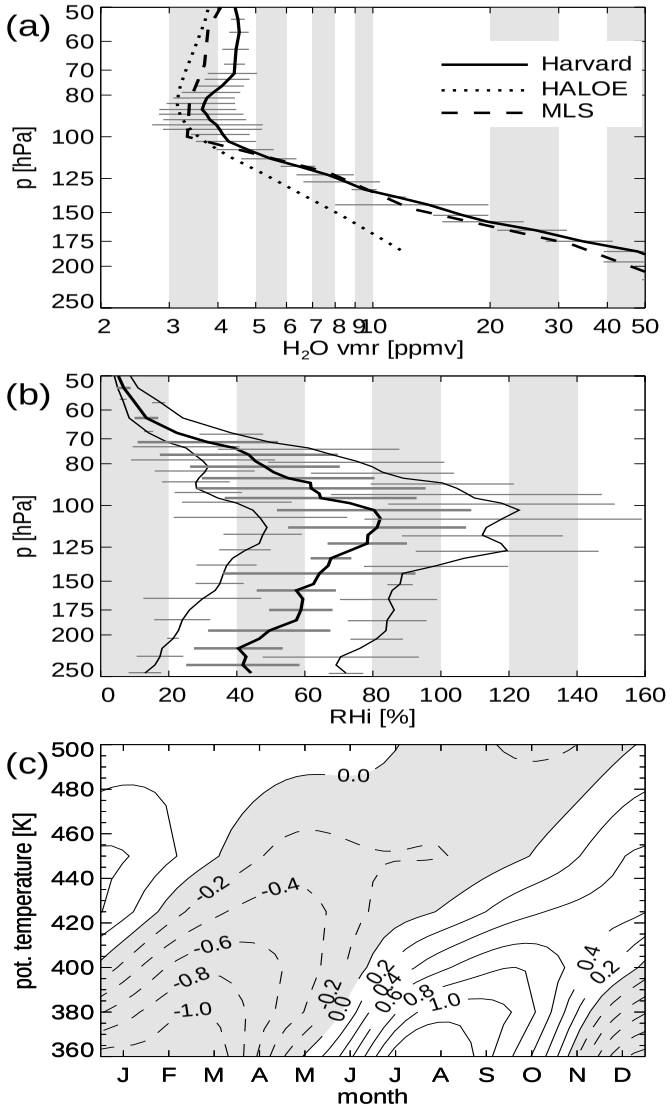

Figure 8: Water vapour profiles. Fueglistaler *et al.*, 2009.

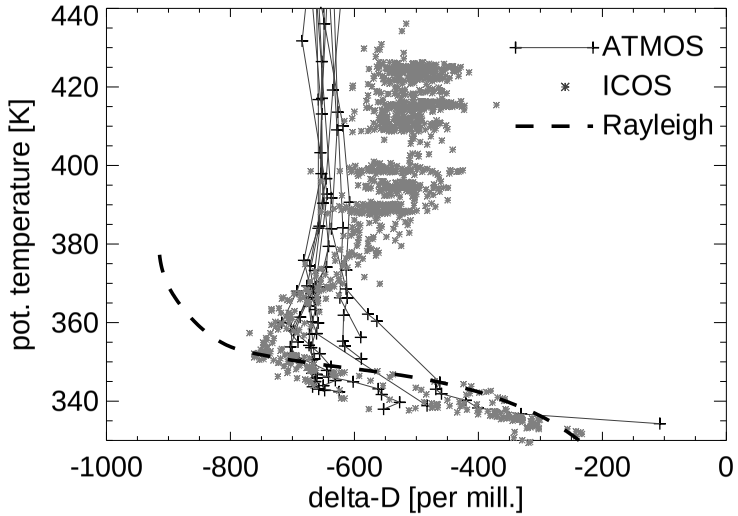

Figure 9: Deuterated water (HDO) profiles; expressed in common 'delta'-Notation. Fueglistaler *et al.*, 2009.

1.5 Clouds

Observation

Measurements of 'clouds' are plagued by differences between instruments as to what they measure, and consequently when and where they 'see' a cloud. A fair estimate of cloud tops (but not what's happening below!) is given by downward looking lidars, such as the CALIPSO measurements, of which we show some measurements here). An important additional factor is time of observation - in particular convection often has a pronounced diurnal cycle, and imcomplete sampling of the diurnal cycle can produce biased results.

Cloud top heights show a maximum in the tropics around 14km, wherease the subtropics show only sparse cloud cover (reflected also in RH-distributions discussed later).

Optically thin clouds (even subvisual) clouds in the TTL

Because of the low vapour pressure, temperature perturbations may lead to formation of 'clouds' with very little condensate, such that the resulting cloud may even be 'subvisual'.

There are interesting questions regarding the formation and maintenance of these clouds, and their net impact on stratospheric humidity (through incomplete sedimentation) is not well quantified currently.

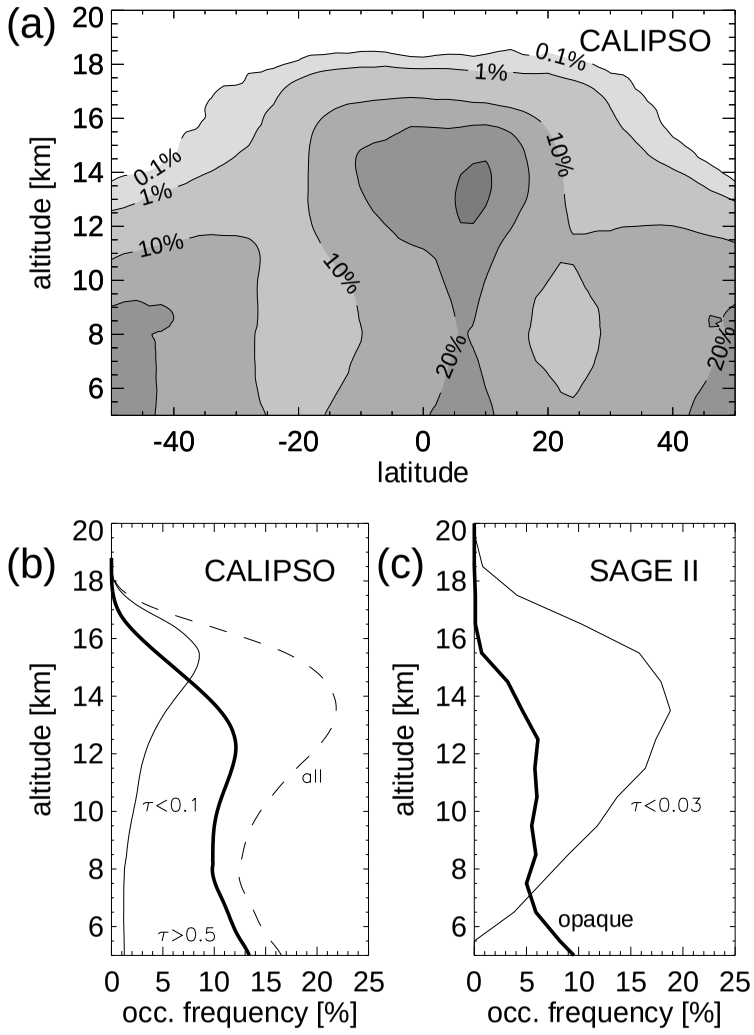

Figure 10: Clouds top distributions, and separation according to optical thickness, from Fueglistaler *et al.*, 2009..

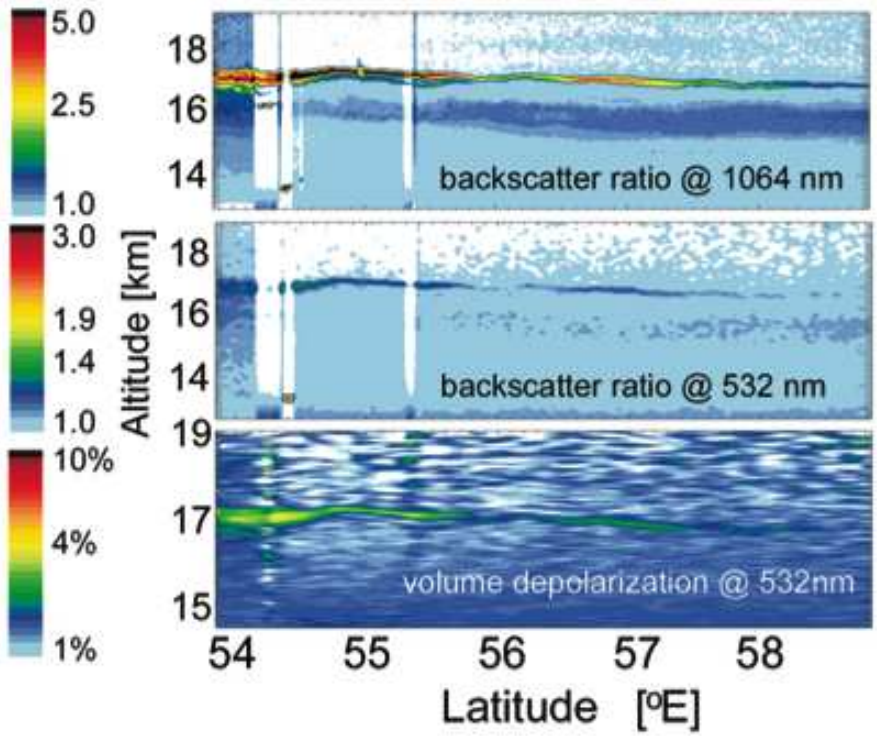

Fig. 5. Lidar measurements during another APE-THESEO flight on 27 February 1999. Backscattering ratios at 1064 nm and 532 nm and volume depolarization at 532 nm measured by OLEX on the Falcon.

Figure 11: Fig. 5; Peter et al. (2003). Note that x-axis is longitude, not latitude. Clouds like this were observed with as little as 40ppbv in the condensed phase.

1.6 The TTL - Entrainment layer or first appearance of 'eddy-driven' circulation?

(See discussion in TTL Rev. Geophysics article.)

- Mean heat budget
- Annual cycle
- Tracers
- Timescales (convective turnover times etc.)

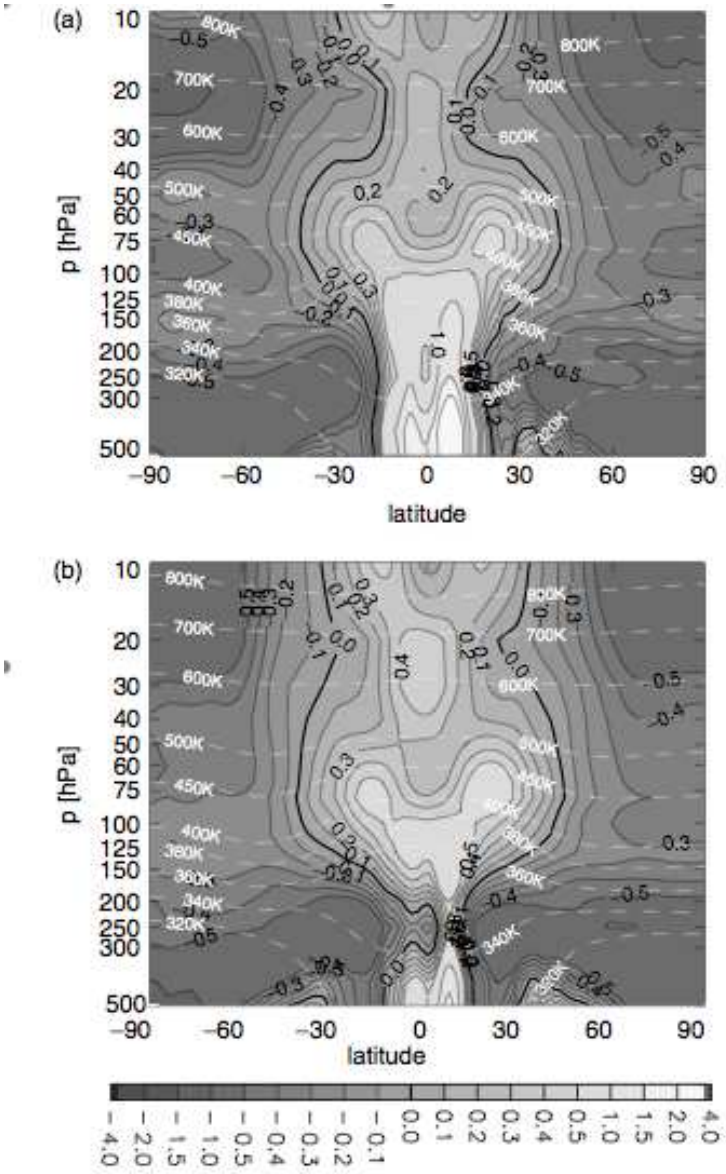

Figure 1. Zonal mean, annual mean (year 2000) total model diabatic heating rates (grey shading, K day^{-1}; zero line bold) from (a) ERA-40 model, (b) ECMWF interim reanalysis model; white dashed contours show potential temperature (K). Note changes in contour spacing to capture full dynamic range.

Figure 12: Fueglistaler, Legras, Beljaars, Morcrette, Simmons, Tompkins, Uppala; QJRMS 2009.

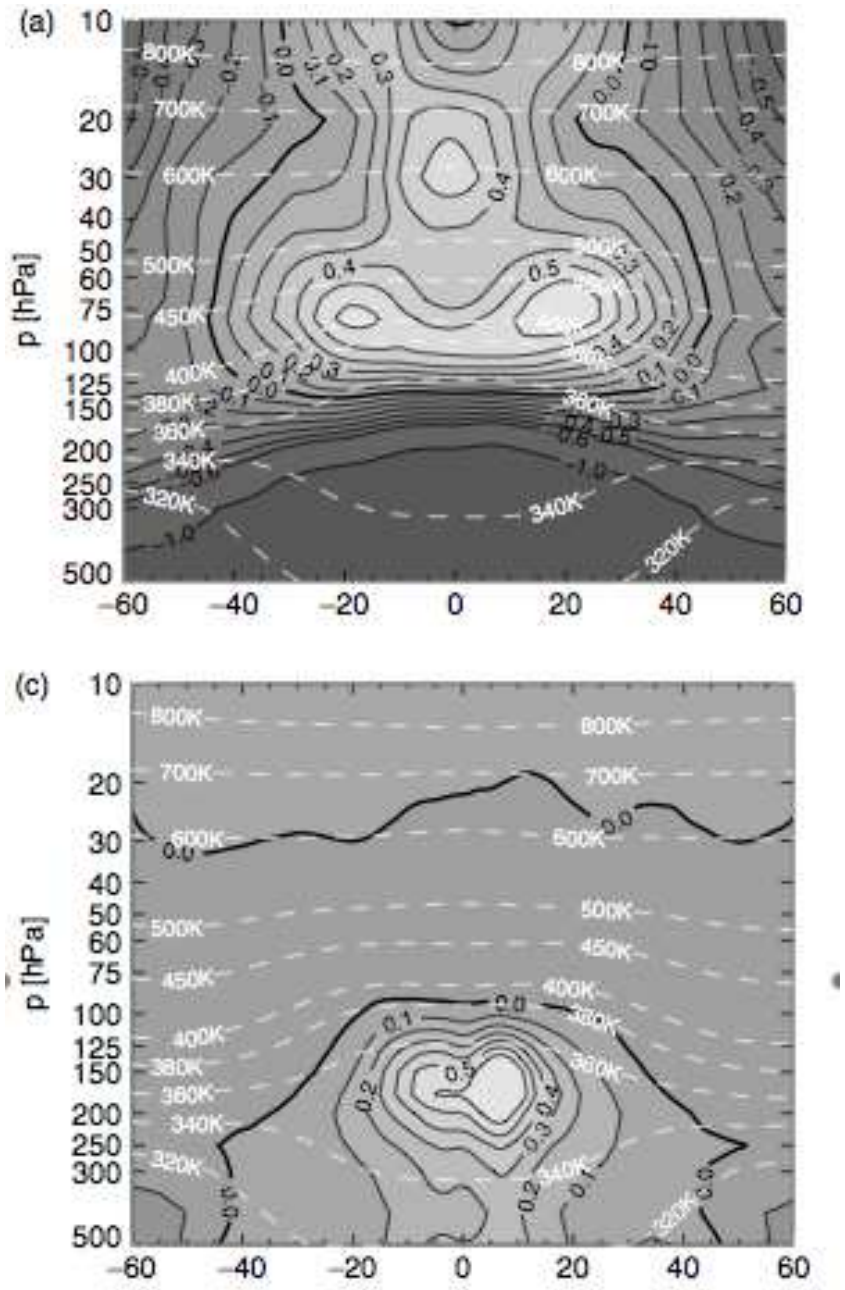

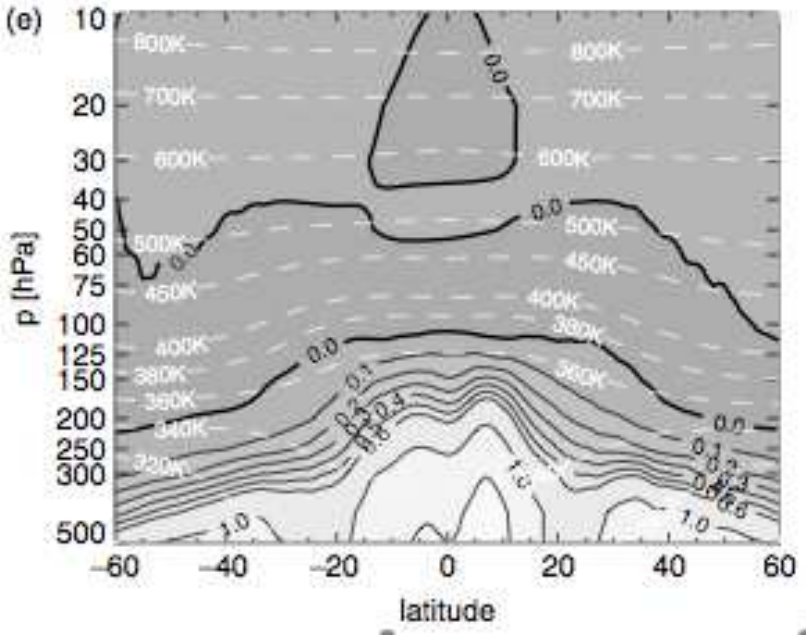

Figure 13: Figure 2; Fueglistaler, Legras, Beljaars, Morcrette, Simmons, Tompkins, Uppala; QJRMS 2009. Top: Clear sky radiation; middle: clouds; bottom: residual (=latent + model parameterizations, e.g. mixing).

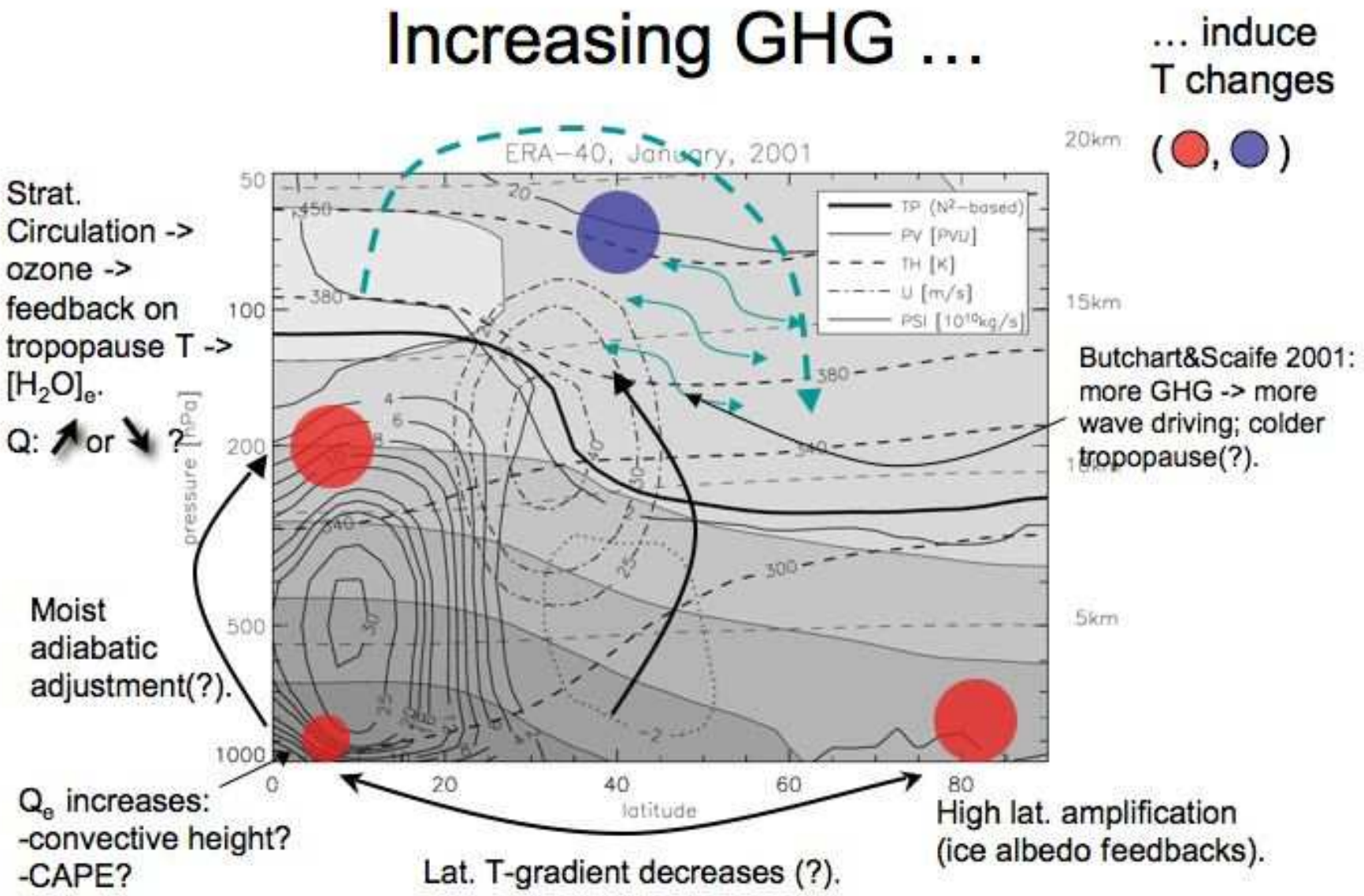
Increasing GHG …
… induce
T changes
(,)
Strat.
Circulation ->
ozone ->
feedback on
tropopause T ->
$[H_2O]_e$.
Q: ↗ or ↘ ?
ERA−40, January, 2001
TP (N²−based)
PV [PVU]
TH [K]
U [m/s]
PSI [10⁹kg/s]
pressure [hPa]
latitude
20km
15km
5km
Butchart&Scaife 2001:
more GHG -> more
wave driving; colder
tropopause(?).
Moist
adiabatic
adjustment(?).
Q_e increases:
-convective height?
-CAPE?
Lat. T-gradient decreases (?).
High lat. amplification
(ice albedo feedbacks).

Figure 14:

2 Dehydration - selected aspects

Lecture overview

In this lecture we discuss particle growth and sedimentation, the quintessential process through which the atmosphere loses moisture (i.e. the sink term). This lecture is also motivated by the observational fact that the amount of condensate in the atmosphere is (surprisingly) small.

Key aspects

The degree to which moisture in excess of saturation is removed depends on the fall speed of the condensate. Any condensate leads to a vertical redistribution of moisture. 'Precipitating' clouds are simply clouds where particles are large enough to reach the ground. Other particles may (re-)evaporate at levels below the initial cloud formation level. In the TTL, in-situ formed ice crystals are small with low sedimentation speeds, such that re-evaporation dominates - albeit at lower levels.

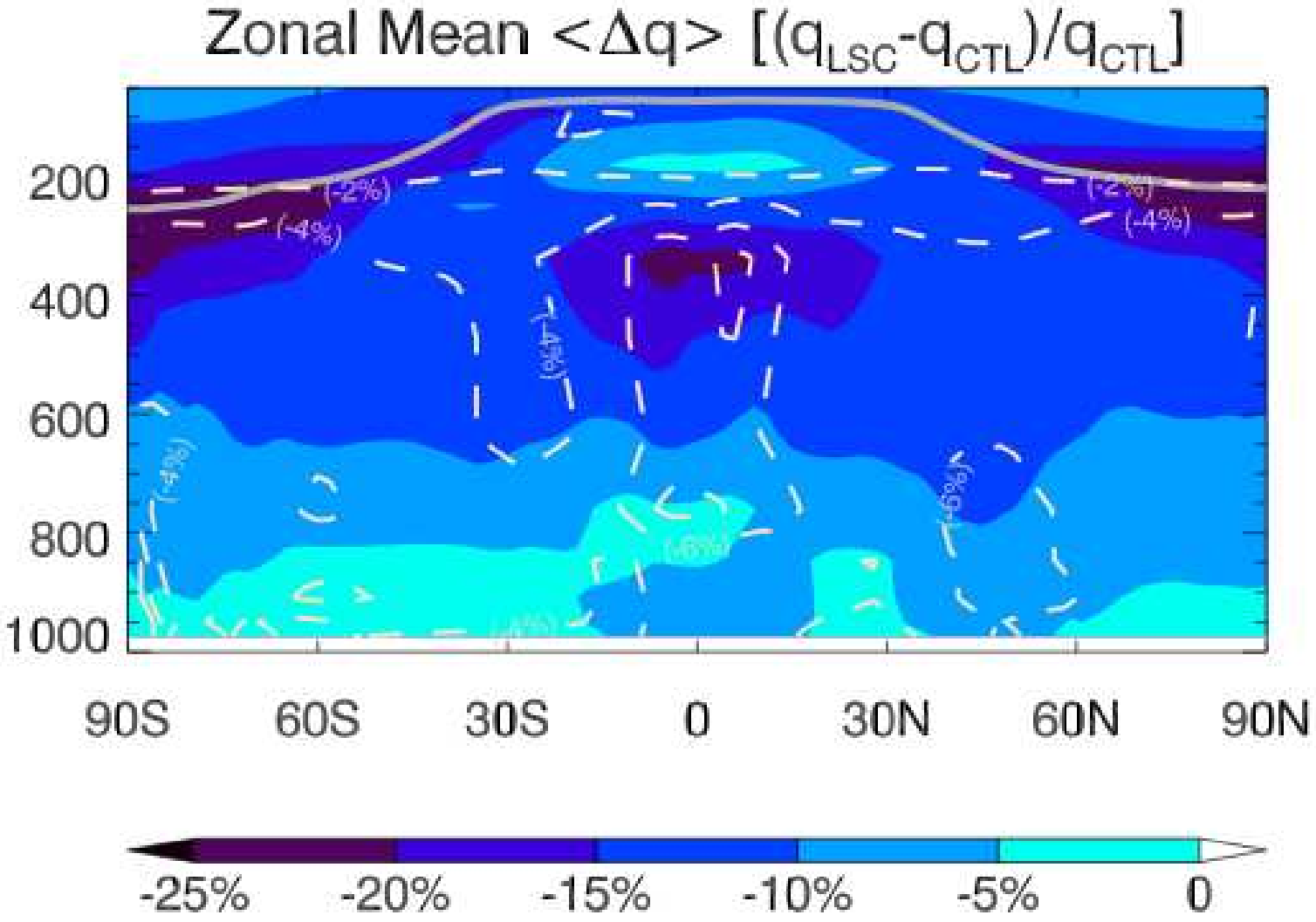

Figure 15: *Wright, Sobel and Schmidt* (2009); Figure 1. Difference in humidity (color coded: absolute, in percent) and relative humidity (white dashed lines) between GCM 'normal water' and additional (dynamically passive) water field where evaporation of condensate is eliminated.

2.1 Nucleation

A few things to remember - details will be covered elsewhere; see also *Pruppacher and Klett* [1997] and *Mullin* [2001].

Nucleation may be classified into primary and secondary nucleation (induced by crystals). Primary nucleation (i.e. nucleation in a pristine solution) may be further divided into homogeneous and heterogeneous nucleation. Homogeneous nucleation requires the nucleation process to occur spontaneous, whereas heterogeneous nucleation describes nucleation induced by foreign particles.

A key quantity for nucleation is the saturation ratio S, given as

$$S \equiv \frac{p_{\mathrm{H2O}}}{e} \equiv \frac{[\mathrm{H2O}]}{[\mathrm{H2O}]_{\mathrm{sat}}} \tag{1}$$

where e is the water vapour pressure (function of temperature; 'Clausius-Clapeyron'), p_{H2O} is the water partial pressure, and [H2O] is the water vapour mixing ratio, with the subscript 'sat' indicating the saturation vapour mixing ratio, as given by

$$[\mathrm{H2O}]_{\mathrm{sat}} \equiv \frac{e}{p} \tag{2}$$

where p is pressure. (Note that we use here 'volume mixing ratios'; the conversion to/from mass mixing ratios is a trivial multiplication with the ratio of the molar weights of water (0.018kg/mole) and air (about 0.029 kg/mole). If particles are present, they will grow when $S > 1$ and shrink when $S < 1$.

- Nucleation often has to overcome a nucleation barrier/threshold. For homogeneous nucleation, a sensible value to remember is S=1.6; see *Koop et al.,* [2000].
- Vapour pressure (Clausius Clapeyron) is a function of temperature only: e(T); the basic functional form is $e(T) = e(T_0) \cdot \exp -1/T$.
- Water droplets may be substantially supercooled (i.e. they do not freeze despite the ice phase being thermodynamically more favourable), leading to ambiguity with respect to the relevant vapour pressure curve.

2.2 Diffusive growth of spherical particles

Particles can change their mass due to the following processes. (a) Coalescence: particles collide and may form larger particles; (b) Breakup: mechanical stress may lead to breakup of particles; (c) Mass flux between the particle and the surrounding gas/liquid phase if the particle and the surrounding gas/liquid are not in thermodynamic equilibrium. (I.e. $S \neq 1$.)

Here, we focus on process (c) - mass exchange between the particle and surrounding gas phase. Under the assumption that the density of species i in the gas phase is continuous up to the drop surface, the diffusion equation describes the mass exchange between particle and gas phase. In cases where this assumption breaks, e.g. when the particle size is comparable to the mean free path of the air molecules, the diffusion equation must be corrected [*Pruppacher and Klett* 1997]. This correction is of practical importance mainly for aerosol and clouds in the stratosphere (because of small particles, and low pressure in the stratosphere), and may be neglected in many cases in the context of tropospheric clouds.

In practise, analytical solutions are available only for simple particle geometries. In the case of a spherical particle/drop,

$$\frac{da}{dt} = D_{vap} \cdot \frac{M_w}{R \cdot T \cdot \rho_w} \cdot (p^{\mathrm{part}} - p^{\mathrm{vap}}) \cdot \frac{1}{a} \tag{3}$$

describes the change in radius due to diffusion; where:

a: Radius of the particle.

D_{vap}: Diffusivity (of water vapour in this case).

M_{w}: Molar mass of water

R: Ideal gas constant.

T: Temperature.

ρ: Density of condensate.

$p^{\text{part}}, p^{\text{vap}}$: Partial and vapour pressure.

Even for this simplest case we note two corrections (for details please see Pruppacher and Klett):

Ventilation: A falling particle experiences 'ventilation'; this is accomodated for with a 'ventilation coefficient' (being the ratio between mass growth at finite velocity and that at rest), which in turn depends on the "Schmidt number" and the "Reynolds number".

Kelvin effect: Correction of the vapour pressure for a curved surface. (A function of the surface tension.)

A convenient form to write the equations of diffusive growth is

$$\frac{\mathrm{d}m}{\mathrm{d}t} = G \cdot 4\pi\rho_w \cdot \Delta p \cdot a \tag{4}$$

$$\frac{\mathrm{d}a}{\mathrm{d}t} = G \cdot \Delta p \cdot a^{-1} \tag{5}$$

where

$$G = D(T) \cdot \frac{M_w}{RT\rho_w} \tag{6}$$

$$\Delta p = p^{\text{part}} - p^{\text{vap}} \tag{7}$$

Hence, the growth of aerosol particles is proportional to a 'growth term' G and the difference of vapor pressure and partial pressure.

For aspherical particles the growth term may be adapted to:

$$G^* = G_{\text{sphere}} \cdot \frac{C}{a_{\text{es}}} \tag{8}$$

where C is the capacity of the shape (see table **??**) and a_{es} is the radius of the mass-equivalent sphere.

The ventilation of spherical particles can be taken into account with a ventilation coefficient, such that the growth term can be written as:

$$G'_{\text{sphere}} = G_{\text{sphere}} \cdot \bar{f}. \tag{9}$$

2.3 Sedimentation of small ice crystals

The motion of aerosol in the atmosphere is controlled by gravity and drag of the surrounding gas phase. While the force that gravity excerts on the particle is simply proportional to the mass of the particle, the drag can be calculated analytically only for a few highly idealized particle shapes such as spheres. In addition, classical calculation of the drag force assume the gas phase to be a continuum. This assumption is for sub-micron particles not valid and a correction has to be applied (the so called 'slip-flow correction').

The drag is also dependent on the speed of a particle. For sufficiently slow speed, the flow of the air around the particle is laminar. Increasing the particle's speed will inevitably lead to turbulence at some point, which increases the particle's drag.

For small Reynolds numbers (relative importance of the advection term $\vec{u} \cdot \nabla \vec{u}$ to the linear viscous acceleration term $\nu \cdot \nabla^2 \vec{u}$ in the *Navier-Stokes* equation), one can derive an analytical solution for the fall velocity of spheres.

2.3.1 Terminal fall velocity of spheres in the Stokes-Cunningham regime

The drag on a sphere in a Stokes flow is:

$$D_S = 6\pi a \eta U_\infty \tag{10}$$

and we obtain for steady-state conditions (drag balances gravitational acceleration):

$$6\pi a \eta U_\infty = \frac{4}{3}\pi a^3 \cdot g(\rho_{\text{drop}} - \rho_{\text{air}}) \tag{11}$$

where ρ_{drop} is the density of the drop and ρ_{air} is the density of air (or any other gas/liquid). It follows for the terminal fall velocity for a sphere in the Stokes-Cunningham regime:

$$\boxed{u_{Stokes} = \frac{2 \cdot g \cdot (\rho_{\text{air}} - \rho_{\text{aerosol}})}{9 \cdot \eta} \cdot a^2} \quad \text{for : negligible Reynolds numbers} \tag{12}$$

where g is the gravitational acceleration, ρ_{air} is the density of air, ρ_{aerosol} is the density of the aerosol particle, η is the viscosity of air and a is the particle radius.

A convenient form to write equation 12 is:

$$\boxed{\frac{dz}{dt} = S \cdot a^2} \tag{13}$$

where a is the particle radius and S is the 'sedimentation term', defined as:

$$S \equiv \frac{2g\triangle\rho}{9\eta} \quad [\text{m}^{-1}\text{s}^{-1}] \tag{14}$$

and g is the gravitational acceleration, $\triangle\rho$ is the density difference of particle and surrounding medium and η is the viscosity.

2.3.2 Other regimes

The calculation of the fall speed of a particle with a more realistic shape and/or in a regime of larger Reynolds numer gets quickly very complicated, and can, in general, be solved only numerically.

The main point to remember here is that particle growth and fall speed are related to particle size, and consequently the exact calculation of the gravitationally settling mass flux is most challenging.

2.4 Conceptual and simplified models

The calculation of the sedimenting 'water' flux is very challenging. As we have seen, the fall velocity depends critically on the size and shape of the particles. Bearing in mind that in reality the particles show a spectrum of sizes (and shapes), it is easily seen that an accurate calculation would be numerically very challenging (In fact, the only way for an accurate calculation is to track the size and position of individual particles; as done for a study of sedimenting particles in the stratosphere [Fueglistaler et al., 2002]).

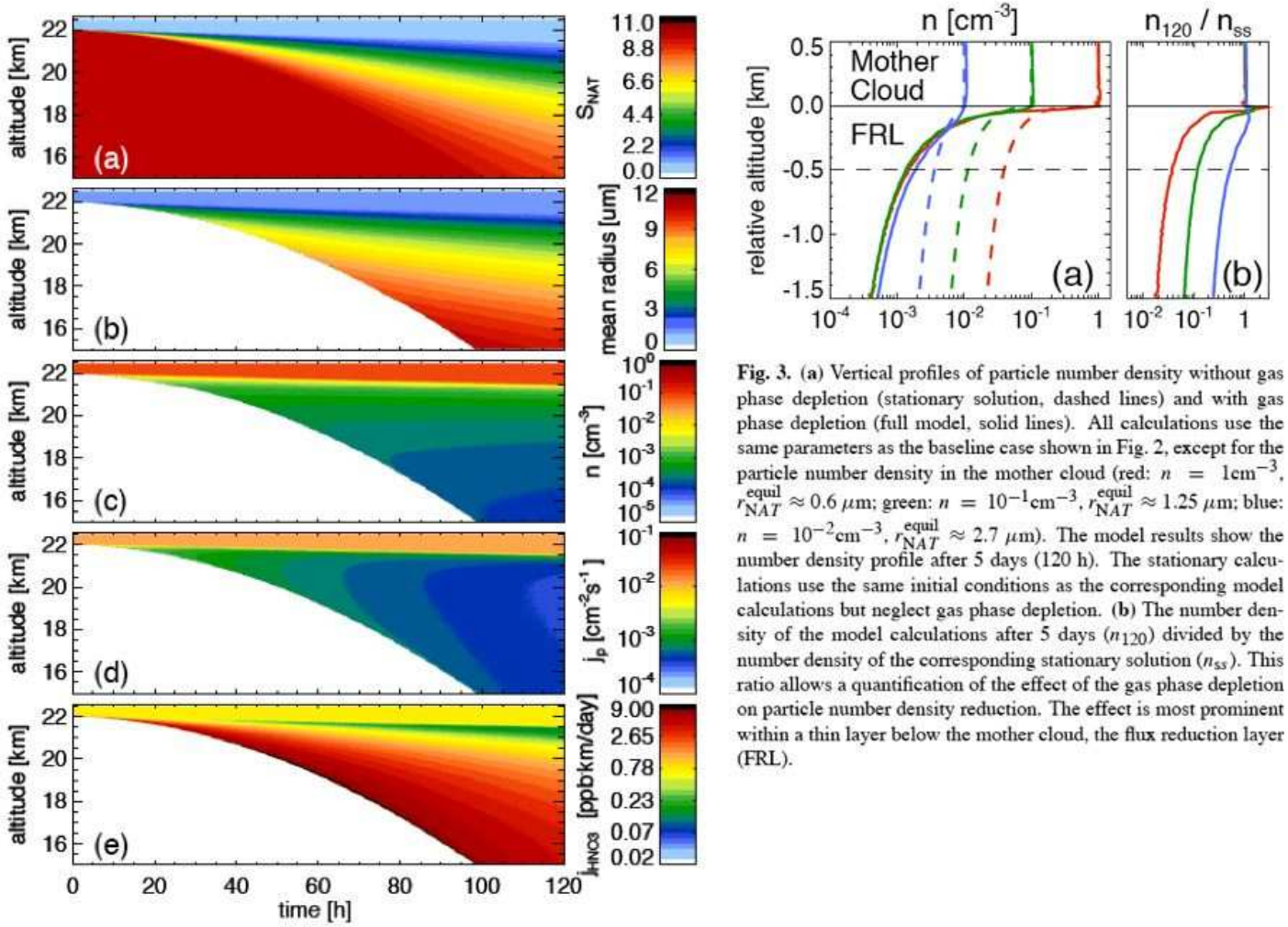

Fig. 3. **(a)** Vertical profiles of particle number density without gas phase depletion (stationary solution, dashed lines) and with gas phase depletion (full model, solid lines). All calculations use the same parameters as the baseline case shown in Fig. 2, except for the particle number density in the mother cloud (red: $n = 1\text{cm}^{-3}$, $r_{NAT}^{equil} \approx 0.6\ \mu\text{m}$; green: $n = 10^{-1}\text{cm}^{-3}$, $r_{NAT}^{equil} \approx 1.25\ \mu\text{m}$; blue: $n = 10^{-2}\text{cm}^{-3}$, $r_{NAT}^{equil} \approx 2.7\ \mu\text{m}$). The model results show the number density profile after 5 days (120 h). The stationary calculations use the same initial conditions as the corresponding model calculations but neglect gas phase depletion. **(b)** The number density of the model calculations after 5 days (n_{120}) divided by the number density of the corresponding stationary solution (n_{ss}). This ratio allows a quantification of the effect of the gas phase depletion on particle number density reduction. The effect is most prominent within a thin layer below the mother cloud, the flux reduction layer (FRL).

Figure 16: A case where detailed calculations of particle growth and sedimentation matters: denitrification of the polar vortices. Note the interesting behaviour of particle number density in the cloud.

In practise, parameterisations often tie (ice) particle size to temperatures and/or total condensed mass. Advanced schemes may employ higher order moments, with 'fall' through the model's vertical levels remaining a challenge.

In order to 'understand' the process in the atmosphere, one has to reduce the complexity of the problem. Here, we show one way (many other possibilities exist).

2.4.1 Conceptual models

The two members spanning the range of possible solutions for the sedimentation problem are:

- no fall out: the sedimentation velocity is negligible;

- complete fall out: the sedimentation velocity is infinite.

Depending on the particular problem under consideration, one or the other extreme solution may be a suitable approximation. However, for most real world applications, the 'truth' lies somewhere in between.

The following conceptual considerations apply to cases where, within reasonable accuracy, the concept of an 'air parcel' can be applied; i.e. strong mixing complicates the picture (but does not invalidate it); and so does the existence of a nucleation threshold (discussed below).

The Lagrangian cold point (LCP)

The LCP refers to the coldest (or driest) point an air mass has experienced prior to observation. (To be precise, it should be the 'Lagrangian point of minimum saturation mixing ratio', but in practise the variations in saturation mixing ratio are dominated by temperature (rather than pressure) variations.) The mixing ratio of the LCP provides an estimate for the observed water vapour concentration under the assumption of complete fall out.

Note: The LCP is **always** the driest possible solution, and is always dry biased relative to observations **if** the temperature history is known with sufficient accuracy. (Note: The fact that LCP-estimates are sometimes moist biased should be reason for concern.)

The Point of Last Saturation (PLS)

The point of last saturation takes into account the finite sedimentation velocity; that is, at the position where the air parcel experiences its LCP, condensate is still present and will (re-)evaporate upon subsequent warming. The PLS is always moister than the LCP.

The Point of Last Contact with Condensate (PLCC)

It is possible that particles evaporate in sub-saturated air; this occurs for example when ice crystals fall into (initially clear air) subsaturated layers.

The PLCC is always moister than the PLS.

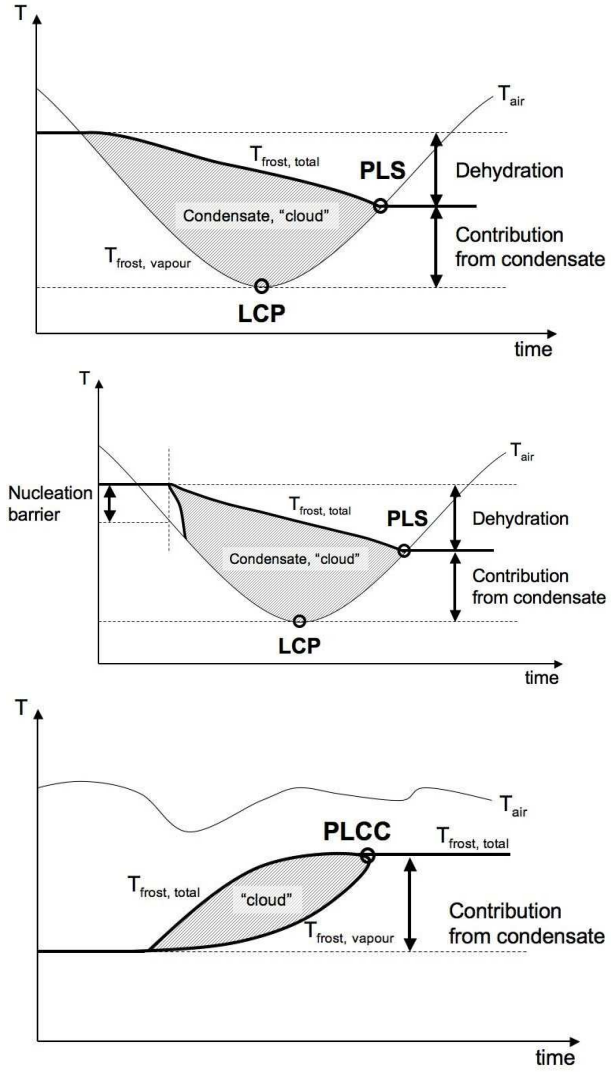

Figure 17: Schematics of the Lagrangian cold point (LCP), Point of Last Saturation (PLS) and Point of Last Contact with Condensate (PLCC). The figure shows the evolution of temperature and frost point temperatures (vapour, and total water) for an exemplary temperature history of an air parcel.

The importance of a nucleation threshold

The presence of a nucleation threshold *always* has a moistening effect relative to the LCP.

For the real atmosphere, the net effect is more challenging to quantify: because of the build-up of supersaturation, the growth of the ice crystals may take a different evolution. (For example, because of higher/lower particle number densities leading to smaller/larger particles; which in turn affect the PLS and PLCC estimates.)

The importance of mixing

Mixing complicates the situation considerably - why? ('Homework')

Is mixing important? Arguments ... ('Homework')

2.4.2 A simple model to estimate the dehydration efficiency

(Results from numerical calculations from Fueglistaler and Baker, 2006.)

Question: How much water is removed from an air mass upon formation of condensate?

Approach: Formulate a simple model assuming there exists a 'temperature history' (as e.g. given from a 'trajectory calculation') of a 'layer' with homogeneous conditions over a certain depth 'h'. The model then calculates growth and sedimentation out of the lower boundary of the 'layer' along the temperature history. Aspects covered:

- With decreasing temperature, more water becomes available, particles grow and fall faster.
- A simple parameterization of particle number density (following Kaercher and Lohmann, 2002) giving higher particle number densities at faster cooling.

Caveat: One must assume a 'layer' with homogeneous conditions and prescribed vertical depth; the problem becomes quite acute after some time into sedimentation: the upper part of the layer may then be in reality free of particles and supersaturation may have to build up prior to formation of new particles. Also, these particles would have a very different size!

Advantage: Conceptually simple.

Model descriptions:

τ_{T}: The timescale of the temperature perturbation - the independent/free parameter.

τ_{fall}: The timescale of fall-out; depends on particle number density and available water (i.e. also on absolute temperature).

P: The scaling parameter $P \equiv \frac{\tau_{\mathrm{T}}}{2\pi\tau_{\mathrm{fall}}}$.

Depending on the value of P, the sedimentation is fast/slow; i.e. for $P < 0.1$ the sedimentation timescale is long compared to the temperature perturbation; and for $P >> 0.1$ ...

F+B2005 note that in the upper troposphere P can easily vary from order 0.01 to 10; i.e. both regimes may be encountered. Further, the coupling of particle number density to cooling rate has a non-negligible impact on P.

The dehydration efficiency

Efficiency: Is a measure how much water is removed from the layer relative to the estimate given by the LCP. Using the previous notation (LCP, PLS):

$$\epsilon \equiv \frac{Q_{\mathrm{PLS}} - Q_0}{Q_{\mathrm{LCP}} - Q_0} \tag{15}$$

where Q is the total water mixing ratio (indexes refer to initial, end, and LCP conditions). That is, $\epsilon = 0$ implies no fall-out, and $\epsilon = 1$ implies complete fall out.

In the presence of a nucleation threshold, the 'speed' does not directly control the efficiency - without nucleation threshold, the faster the dehydration, the more efficient it is. With a nucleation threshold, too fast sedimentation allows additional moisture (in the vapour phase) to escape removal; this is at most exactly the nucleation saturation ratio (minus 1).

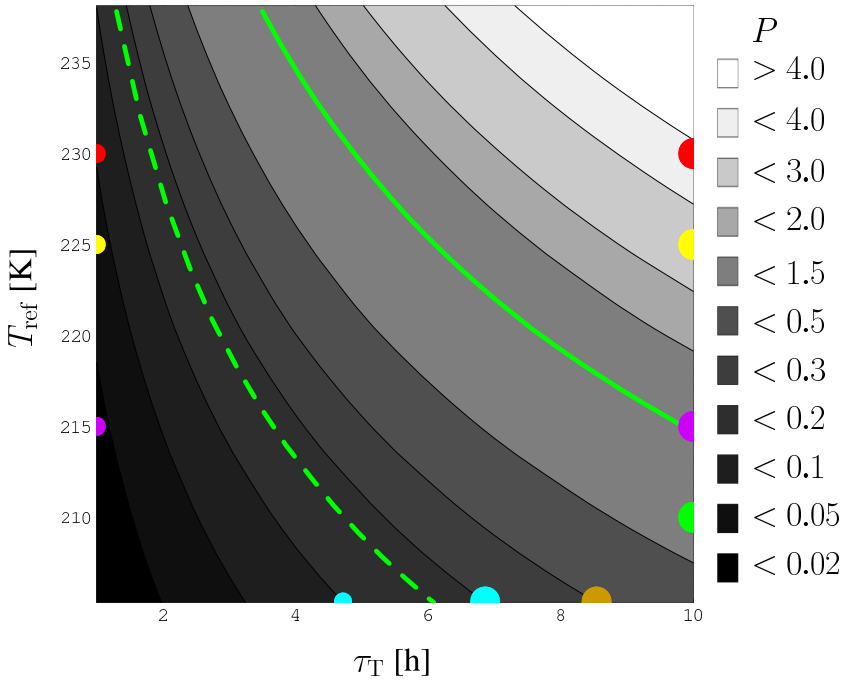

Figure 18: Figure 1 of Fueglistaler and Baker (2006). The non-dimensional parameter P ($P \equiv \frac{\tau_{\rm T}}{2\pi\tau_{\rm fall}}$) as function of $T_{\rm ref}$ and $\tau_{\rm T}$ at $\Delta T = 2K$. Higher P values correspond to lighter gray values. The green dashed curve is $P = 0.16$ and the green solid curve is $P = 1$. Colored dots are the T_{ref}, τ_T values for cases discussed in Section **??**. The P values associated with these dots are as follows: starting from the small red dot on the upper left and moving counterclockwise; $P = .05, .035, .015, 0.1, 0.2, 0.3, 0.64, 1.0, 2.5, 3.8$. Small dots correspond to $P \leq 0.16$ (*slow* regime) and large dots to larger P values (*fast* regime).

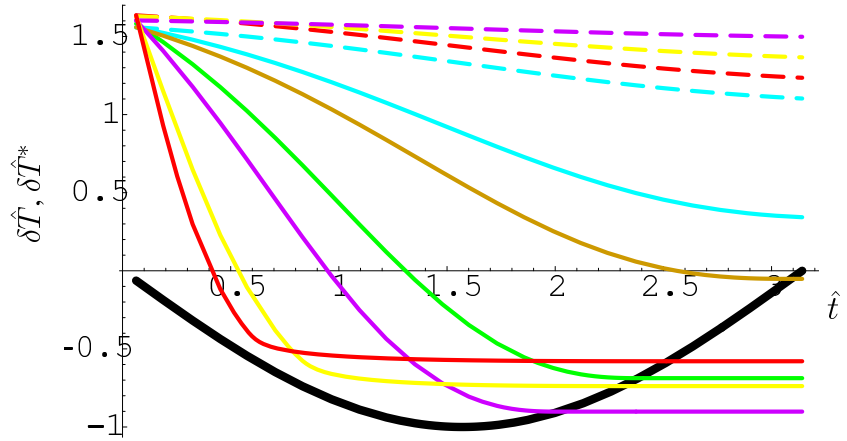

Figure 19: Figure 4 of Fueglistaler and Baker (2006). Evolution of nondimensionalized temperature $\delta\hat{T}(\hat{t})$ (bold black) and of nondimensionalized saturation point temperature $\delta\hat{T}^*(\hat{t})$ over a single cooling event. Each curve corresponds to a ($T_{\rm ref}$, $\tau_{\rm T}$) pair shown by a dot of the same color in Figure 1. Dashed curves correspond to the small dots in that figure and solid curves to the larger ones.

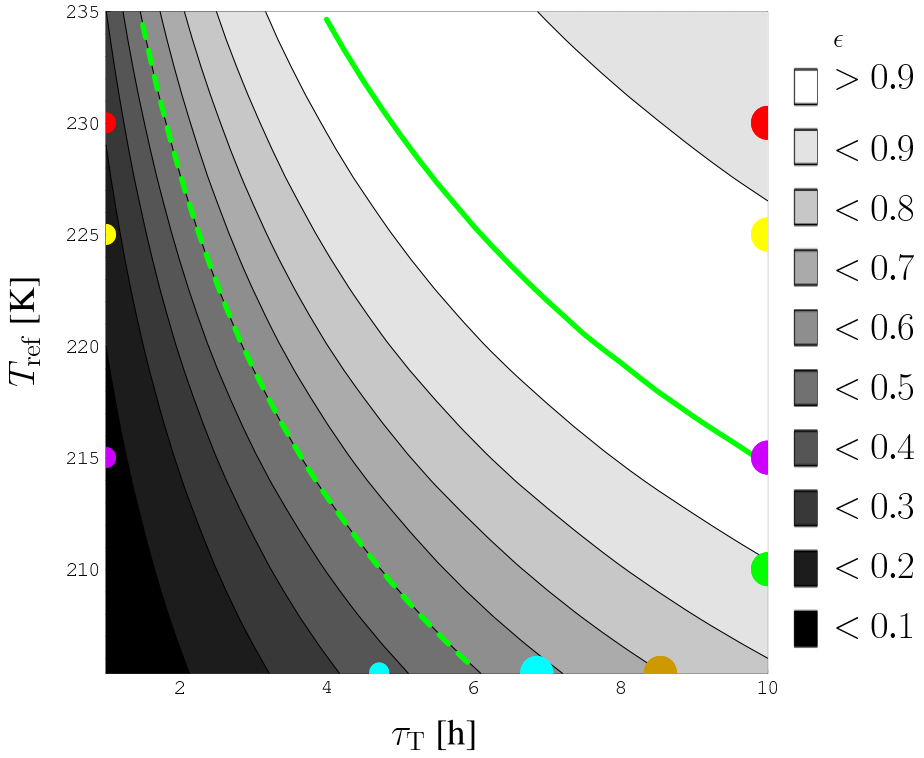

Figure 20: The dehydration efficiency ($\epsilon \equiv \frac{Q_{\mathrm{PLS}} - Q_0}{Q_{\mathrm{LCP}} - Q_0}$). Fueglistaler and Baker (2006).

3 The importance of transport for atmospheric water vapour

Lecture overview

In this lecture we will see that large-scale atmospheric transport is a powerful mechanism for controlling atmospheric water vapour - basically bringing the mean state substantially below concentrations expected from (local) saturation mixing ratios.

We will then study the effect of transport with a simplified 'lab case' derived from the situation encountered in the TTL.

Key aspects

Atmospheric water vapour mixing ratios vary by 4 order of magnitude. Vertical, cross-isentropic transport is the most powerful process (4-OM), followed by quasi-isentropic motion on sloping isentropes (2-OM). Cloud microphysical processes may modify mixing ratios by a factor 2 locally, and even less globally; a result that could be different in 'another world' where more, but smaller ice crystals would occur.

3.1 An overview of the atmospheric moisture distribution

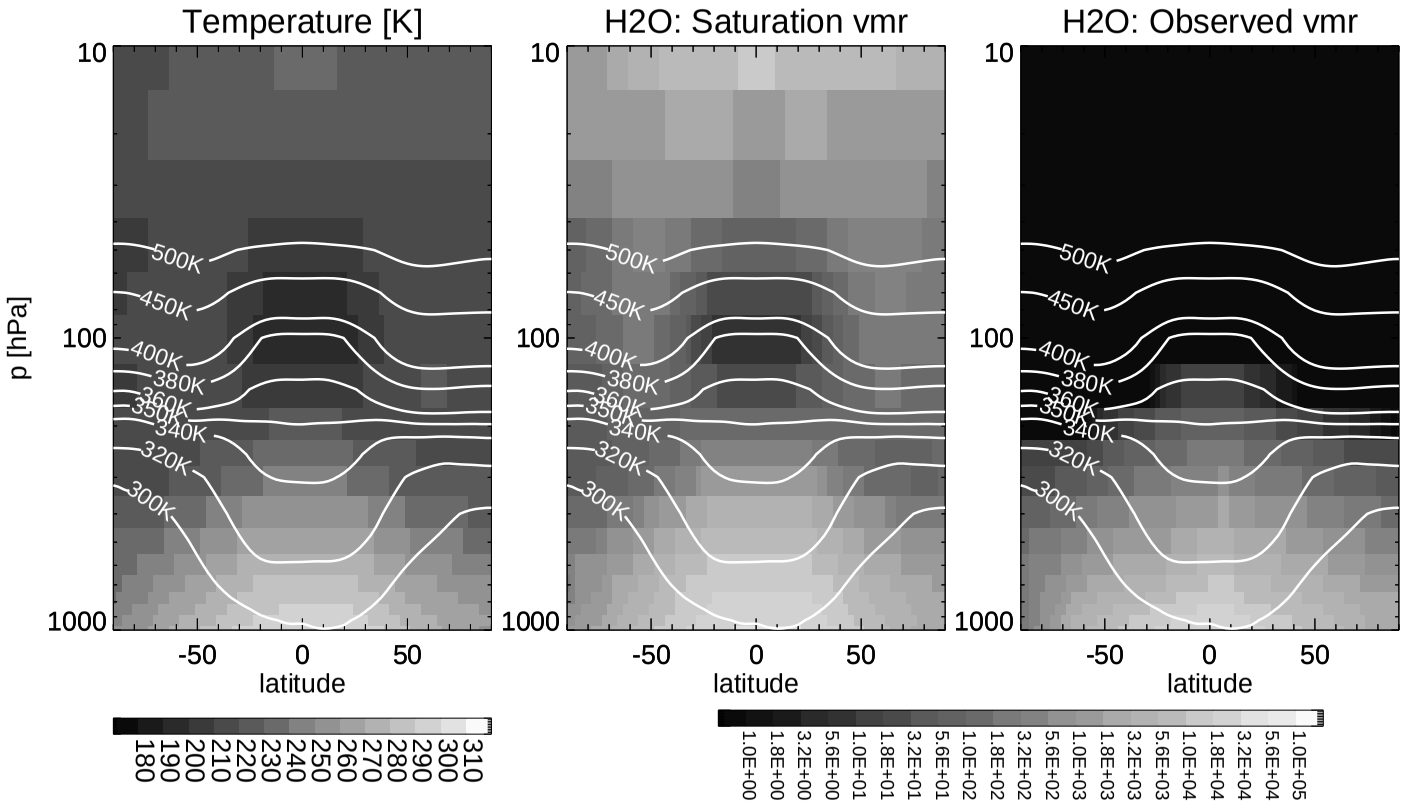

Figure 21: Annnual mean, zonal mean temperature, saturation mixing ratio, and observed water vapour mixing ratios. Data: ECMWF ERA-40, year 2000.

Observation
The atmospheric water vapour distribution follows closely the constraints given by the saturation mixing ratio distribution (which in turn is dominated by the temperature distribution, and modulated by the pressure decrease with height). The most prominent outlier from this rule is the stratosphere. Upon closer inspection (see below), we would also see large deviations in particular in the subtropics.

A closer look at relative humidity distributions

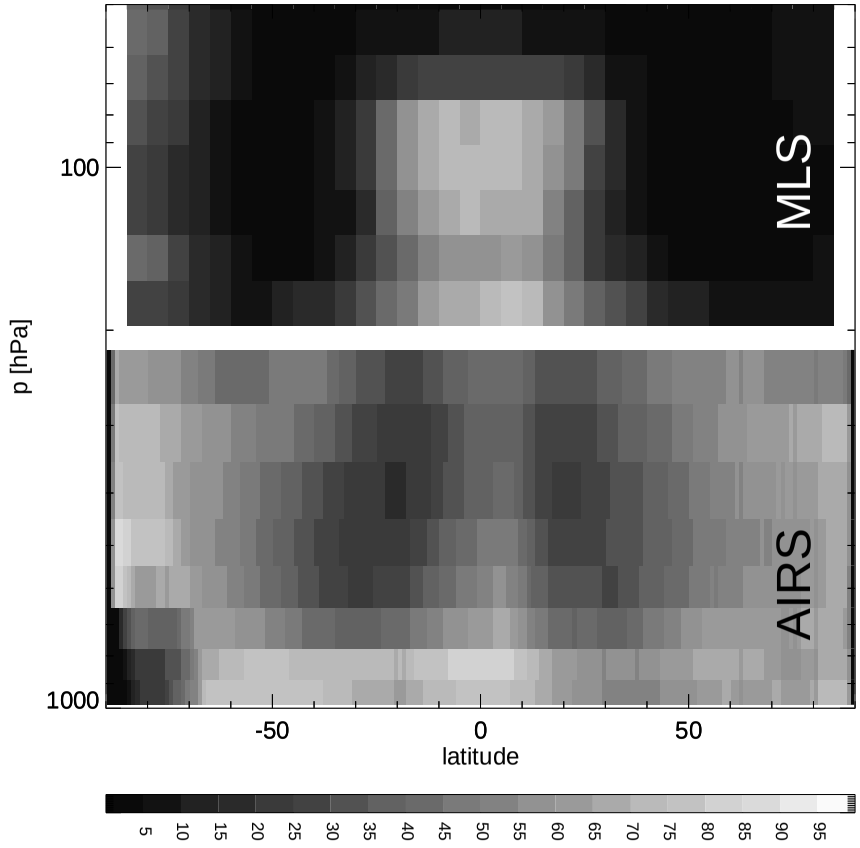

Figure 22: Climatological (2005-2008) mean, annual mean, zonal mean relative humidy distribution as measured by MLS/Aura and AIRS/Aqua. (Data prepared by J. Du, DAMTP; note artefacts due to topography over the South pole.)

Observation
Extremes of relative humidity are found in the TTL (high) and stratosphere (low). Also, as pointed out above, the subtropics show also low relative humidity values.

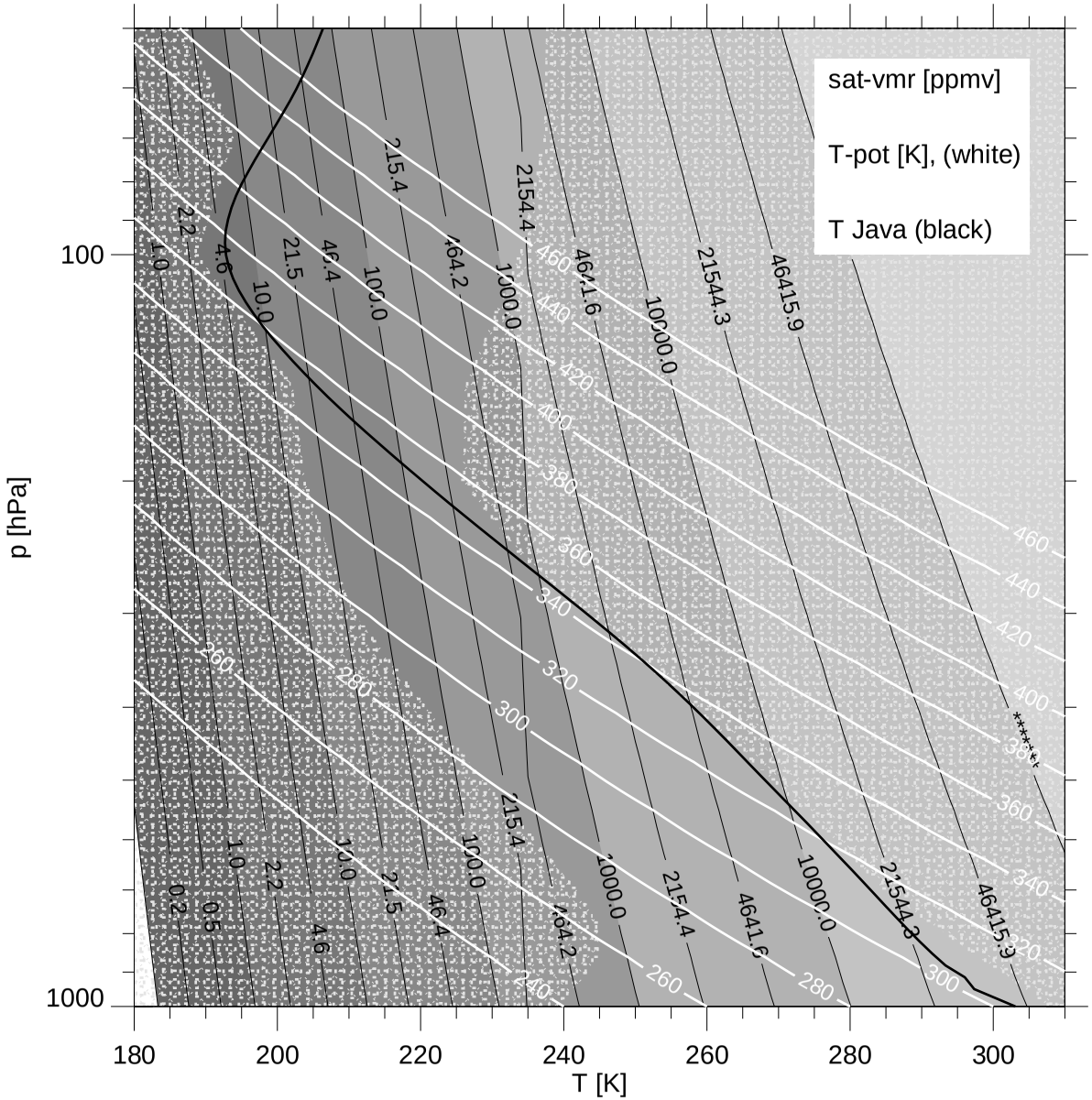

Figure 23: Temperature/pressure diagram (Note: p-axis scaled and oriented as in atmospheric conventions). Hatched area is not realised in atmosphere. Data: ECMWF monthly mean Temperatures for January 2000.

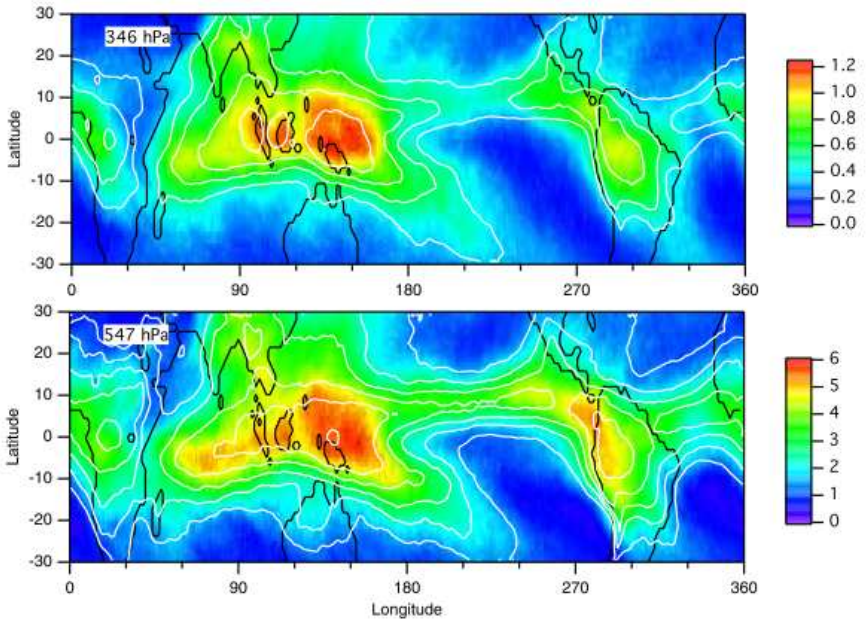

Figure 1. Model-simulated H_2O mixing ratio (g/kg) at 346 hPa (top) and 547 hPa (bottom), averaged from 1 March 2003 to 28 Feb. 2004. White contours are contours of AIRS-measured H_2O in the 400- to 300-hPa layer (top) and the 600- to 500-hPa layer (bottom). In the top plot, the outer contour is 0.4 g/kg and the interval is 0.15 g/kg; in the bottom plot, the outer contour is 1.5 g/kg and the interval is 0.625 g/kg.

Figure 24: Dessler and Minschwaner, 2007.

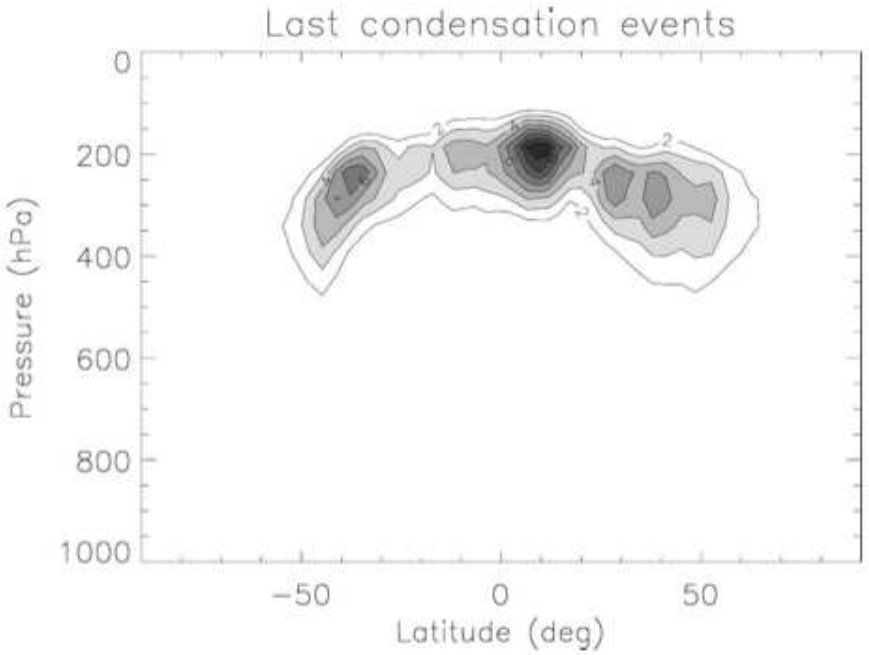

FIG. 4. Density of origin or number density of the last condensation events, summing events at all longitudes and times during January 1993 (277, 189 events), normalized so that integral of (1) over the atmosphere is unity. A value of 10 corresponds to 3625 trajectories experiencing condensation in a zonal box with Δp = 50 hPa and $\Delta\mu$ = 2/45 (4° lat near the equator).

Figure 25: Cau, Methven and Hoskins, 2007.

Discussion

- Vertical cross-isentropic motion can change saturation mixing ratio by 4-OM.
- Quasi-isentropic motion can change saturation mixing ratio by 2-OM.
- Cloud microphysical process may modify actual mixing ratios by about a factor 2 - no justification for estimate given here; globally, it may be even less (see also recent paper by Wright et al., GRL, 2009).
- Low relative humidity indicates absence of 'local' control.

3.2 The case of stratospheric water vapour

The pronounced spatio-temporal structure of the temperature field in the TTL may have profound consequences for the control of water entering the stratosphere. One possibility to analyse this aspect is through trajectory calculations - that is, one traces stratospheric 'air parcels' back to the troposphere, and determines their Lagrangian cold point.

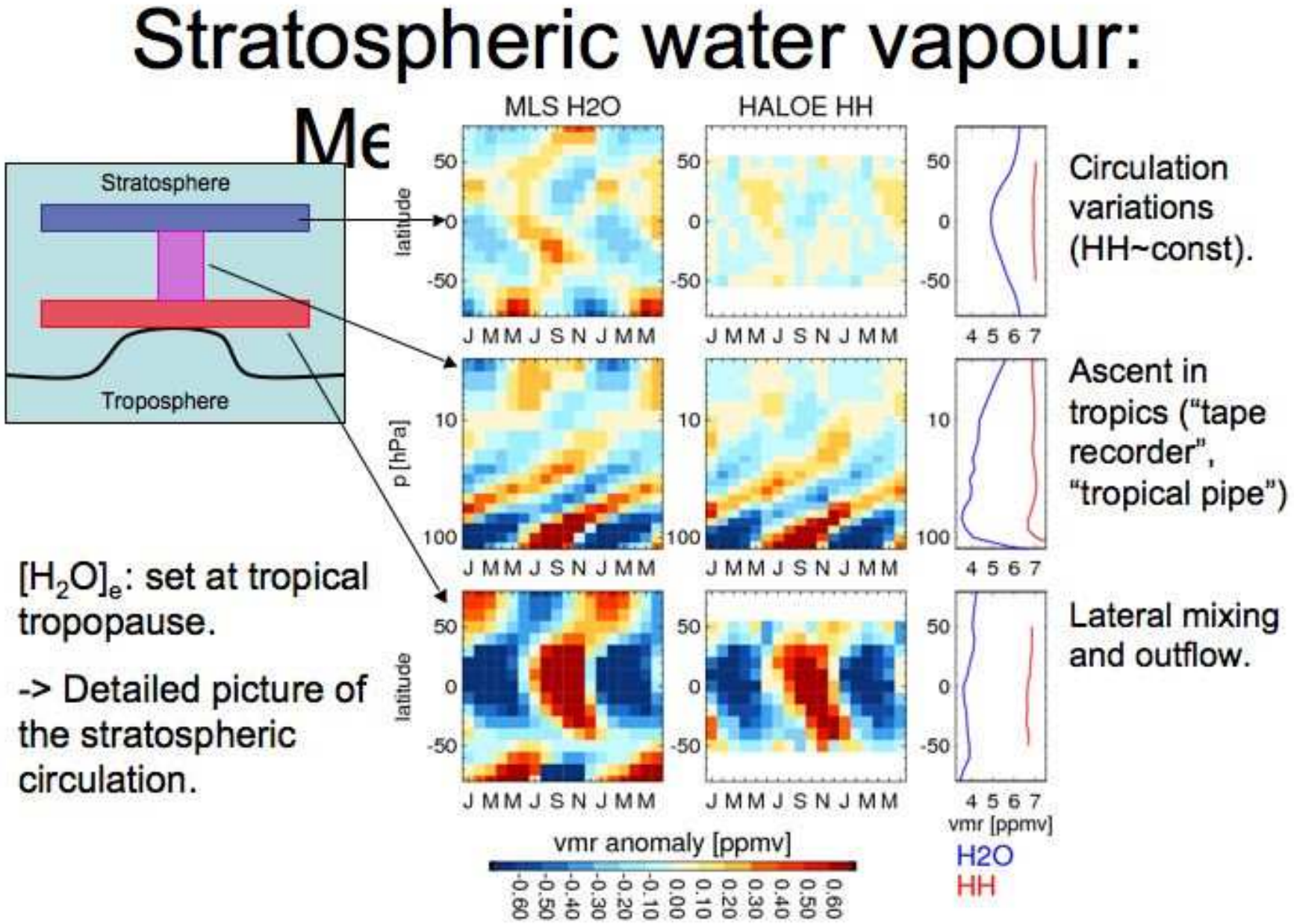

Figure 26: Annual variations of stratospheric water vapour.

3.2.1 Description of pathways

While the entry mixing ratio determined in this way is straightforward to interprete and analyse, describing what trajectories actually 'do' during ascent into the stratosphere is quite challenging. One possibility is presented here - other researchers have come up with different measures.

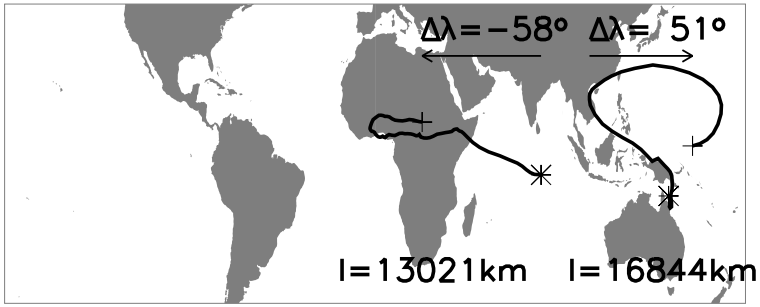

Figure 27: Figure 6 of Fueglistaler et al (2004).

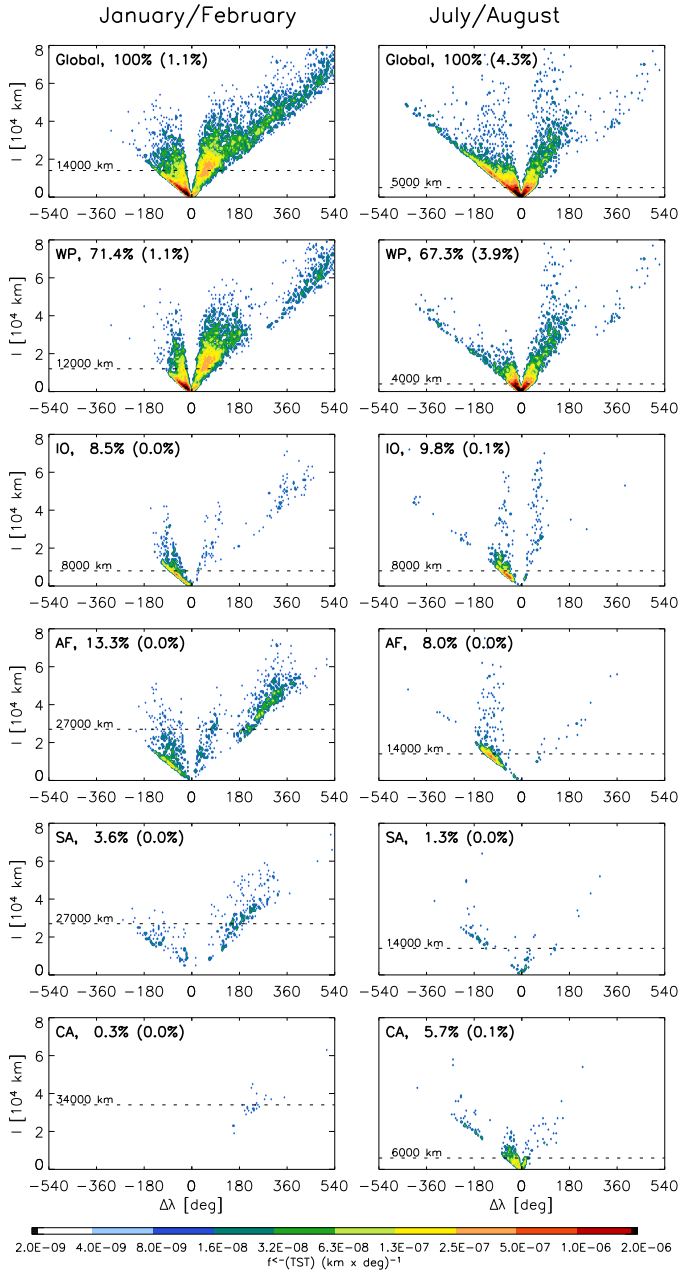

Figure 28: Figure 7 of Fueglistaler et al (2004).

3.3 The Lagrangian cold point distribution

The following figures show results of trajectory calculations based on ECMWF wind/temperature data for tropical troposphere-to-stratosphere transport.

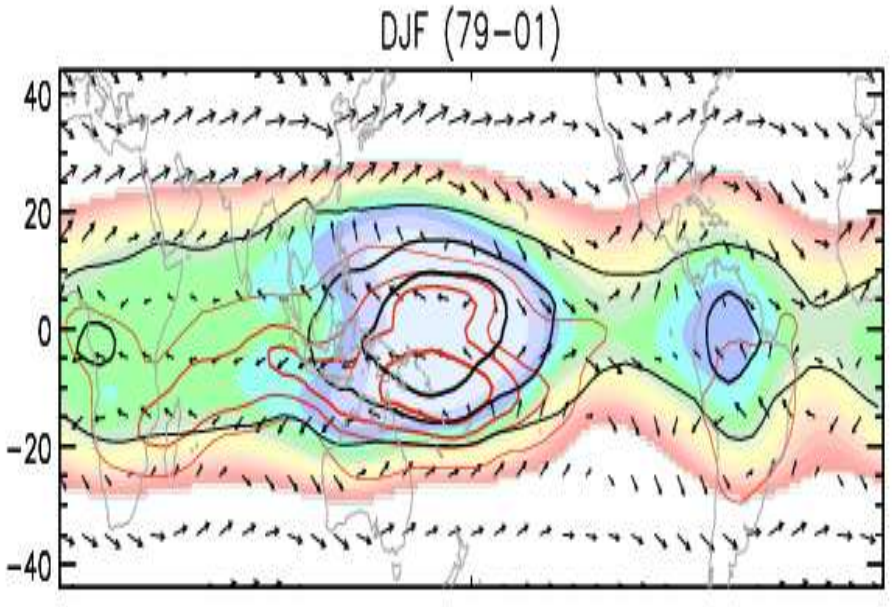

Figure 29: -

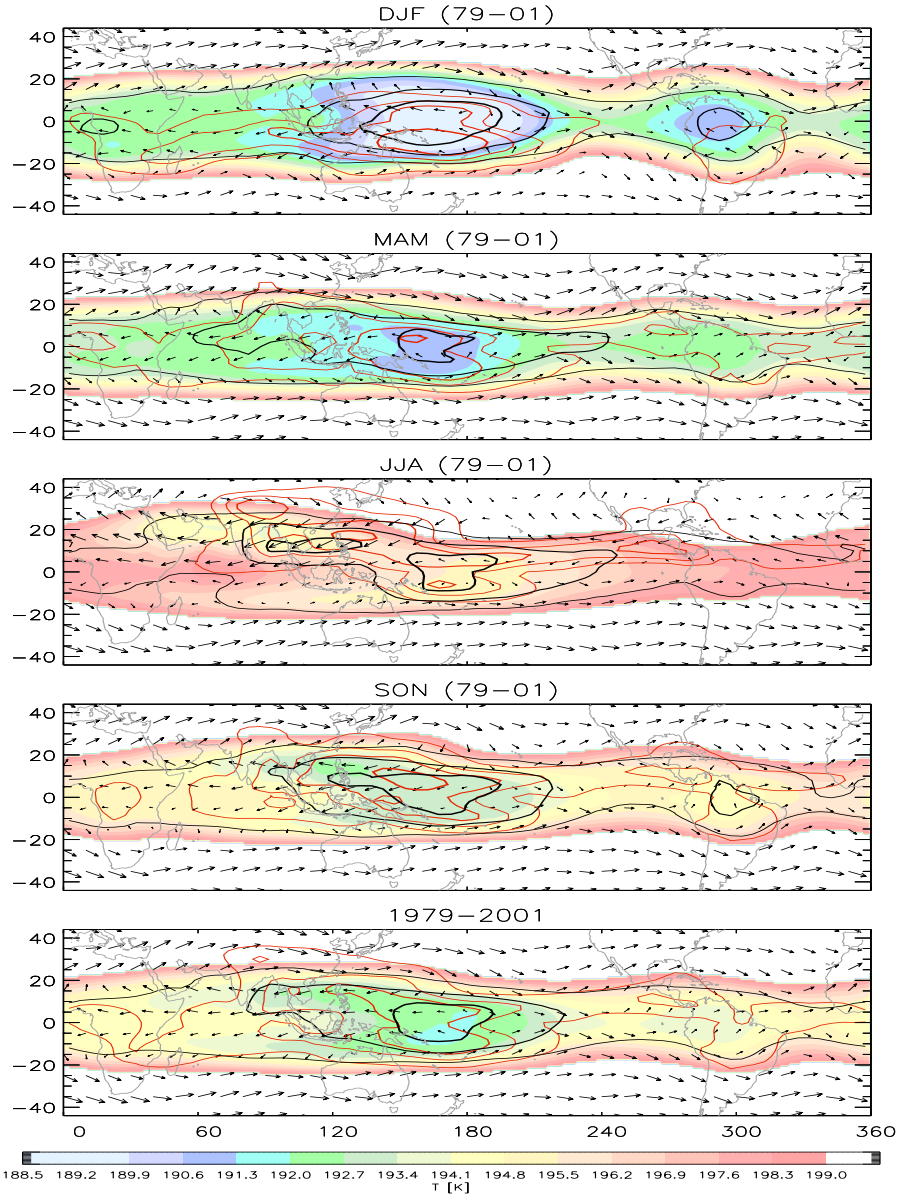

Figure 30: Figure 5 of Fueglistaler et al (2005). The densitiy distribution of the Lagrangian cold point, and that of passing the 340 K isentrope, are shown in black and red contour lines. Color-coded are the mean temperature fields and wind fields interpolated to 90hPa.

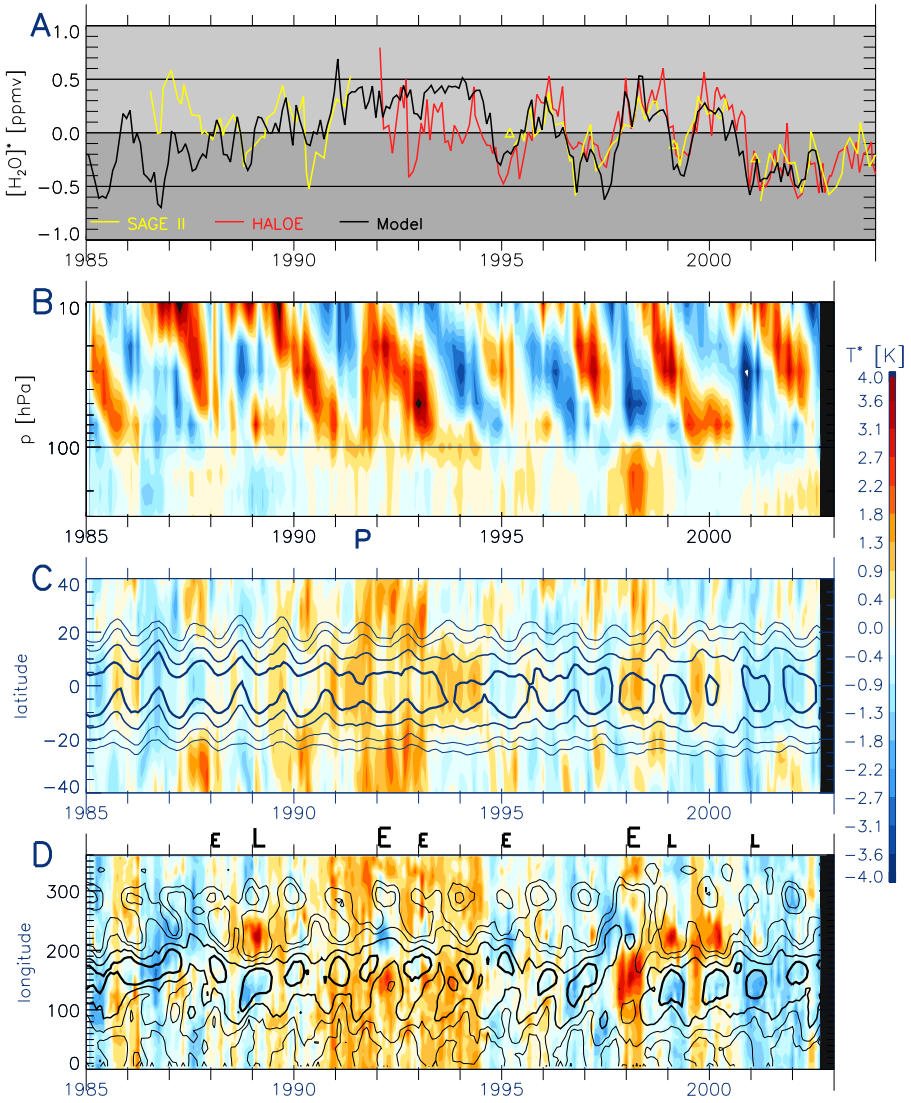

Figure 31: Figure 2 of Fueglistaler and Haynes (2005). (a) Time series of H2Oentry variations; (b) tropical, zonal mean temperature anomalies (after subtraction of the mean annual cycle); (c) Latitude-time structure of zonal mean temperature (after removal of mean annual cycle) and LCP density; (d) ditto, but for zonal structure.

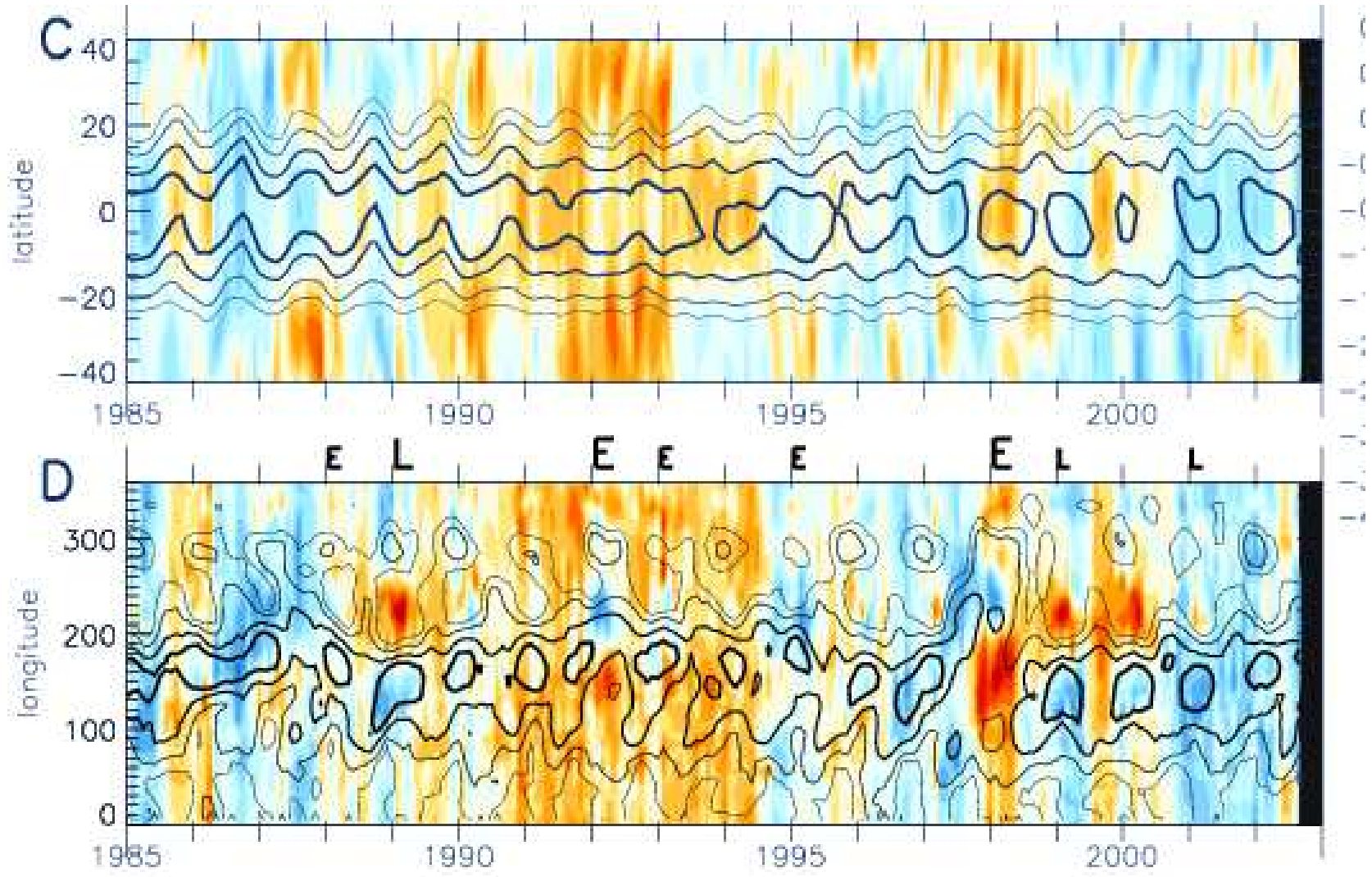

Figure 32: (c) Latitude-time structure of zonal mean temperature (after removal of mean annual cycle) and LCP density; (d) ditto, but for zonal structure.

3.4 The role of ENSO

Impact of ENSO on TST

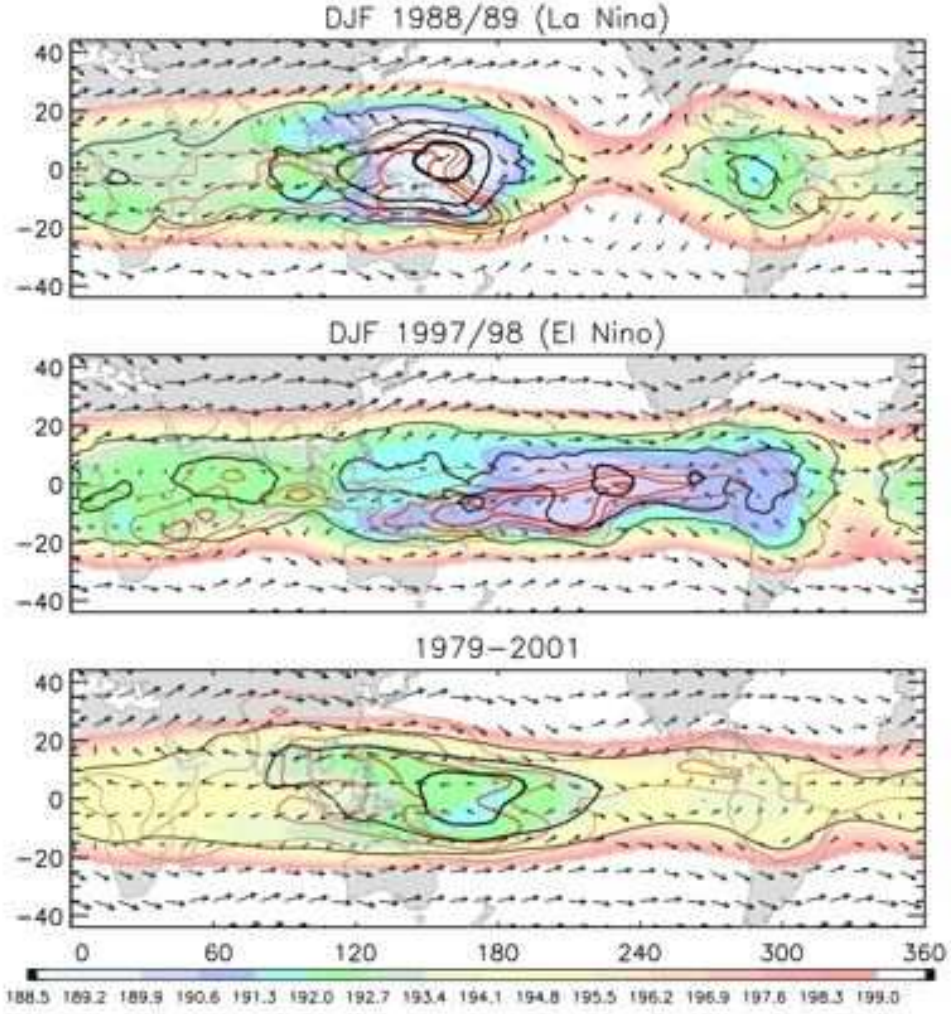

[Fueglistaler et al., 2005]

Figure 33:

ENSO and the Lagrangian cold point distribution

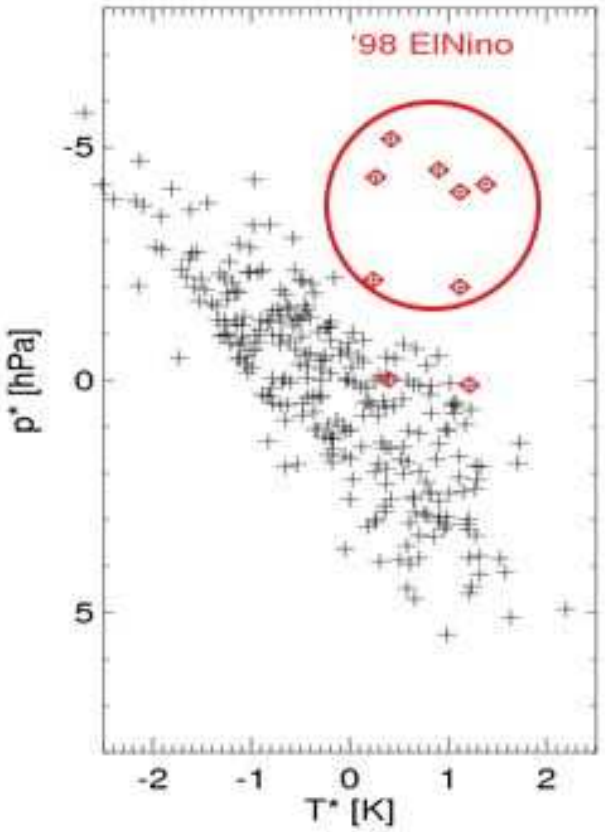

(LCP data from F+H2005)

Variations in Lagrangian cold point temperature and pressure are generally anticorrelated, as may be expected.

Strong 1998 El-Nino is outlier.

Figure 34:

3.5 Stratospheric water vapour variations and trend - a dehydration process-perspective

The stratospheric H_2O trend

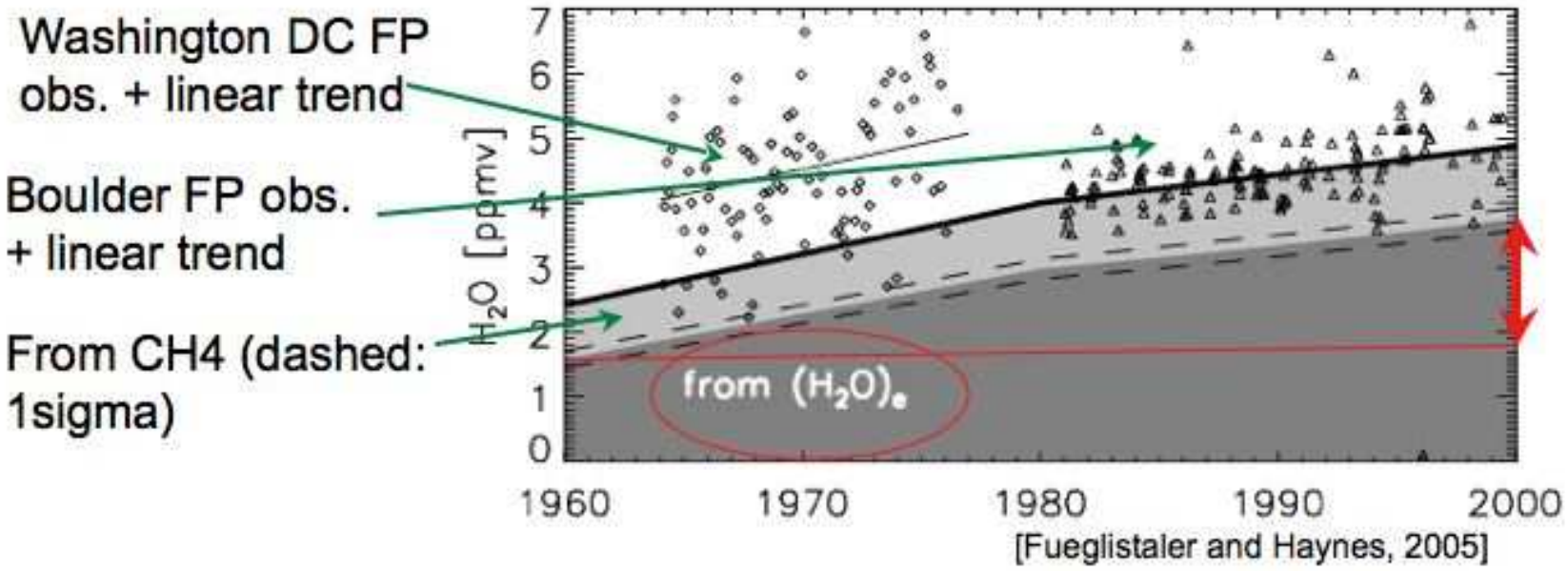

In order to get $[H_2O]e$ for 1960 as suggested by Rosenlof et al. [2001], transport has to decouple the Lagrangian cold point from tropical mean temperatures, inducing a change of **~4 K**.

BUT ...

Figure 35:

The stratospheric H_2O trend

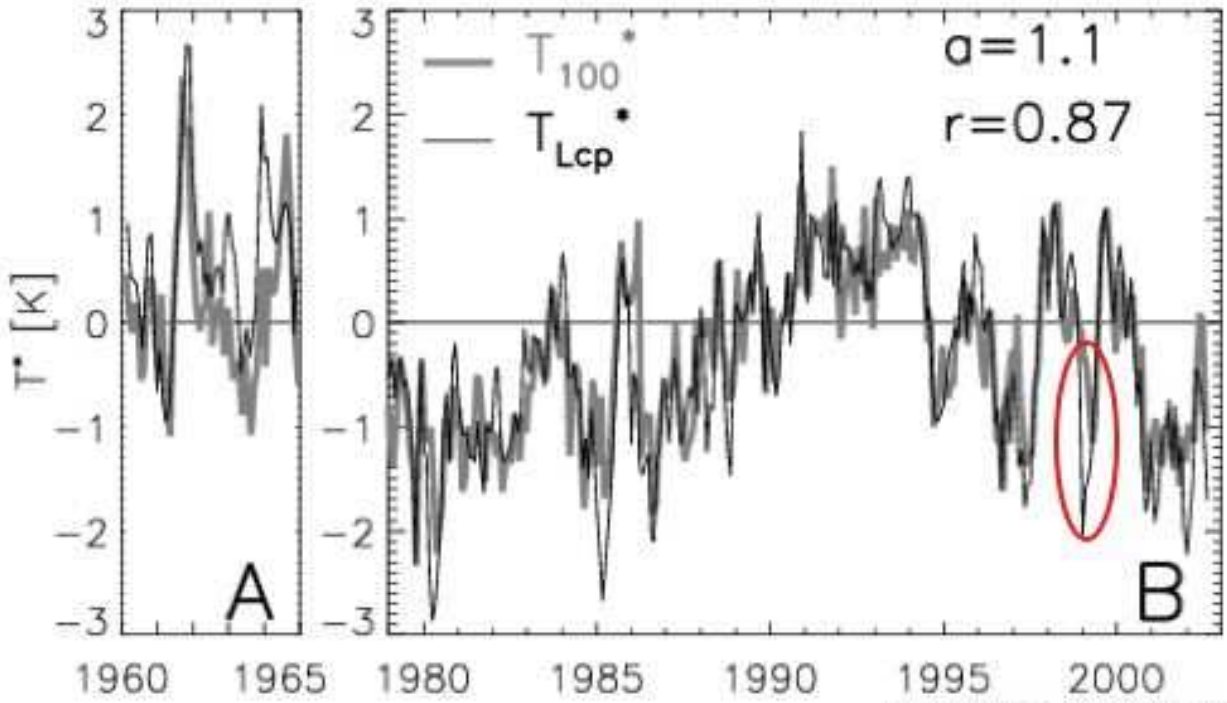

[Fueglistaler and Haynes, 2005]

BUT: Lagrangian cold point is highly correlated with tropical 100hPa temps. for the whole period 1960-2002, which show NO positive trend.

(I.e. neither QBO, ENSO, Volcanoes etc. can explain trend, unless they modify cloud microphysics!)

Figure 36:

Discussion

The Lagrangian cold point calculation is obviously a sensible measure in the case of stratospheric water vapour. This may be somewhat surprising given that the faintest clouds occur in the TTL; but bear in mind that: The smaller the ice content and the smaller the particles, the less efficient is fallout; but at the same time the contribution to the total water decreases.

Newer calculations with less noisy windfields generally show a dry bias, as one would expect. Quantification of the contribution from condensate is exciting ongoing work; perhaps water isotope data can provide additional insights.

The Figure 32 also shows large variations of the LCP-distribution in response to changes in the temperature and wind fields in the TTL (in particular ENSO-related variations). This highlights the importance of a Lagrangian understanding (i.e. dehydration regions are not static, but vary in concert with variations (and trends) of the atmospheric structure and circulation).

4 Hands-on section

Lecture overview

Here, we explore the compex effects of transport on atmospheric humidity with a model with a simplified setup. We take a 2-dimensional (longitude/latitude) wind field and saturation mixing ratio field at the approximate height of the tropical tropopause, combined with a uniform residence time. (I.e. a simplified analogue to transport into the stratospheric overworld.)

Monthly mean wind and temperature data from ECMWF are used, interpolated on potential temperature levels (i.e. the experiments here mimic the effects of isentropic transport). We have prepared 3 different levels - 320K, 345K, and 380K. We will discuss here mainly the 380K level, as this is about the tropical tropopause. However, you are encouraged also to explore the other files.

4.1 The model - Technical information

We provide python-code for the trajectory calculation in 2-dimensions (i.e. u/v) using 1 input wind field and 1 input temperature field (i.e. we ignore temporal fluctuations).

Once you have copied 'stm.tar' to your machine, unpack it (tar xf stm.tar). You will find a collection of python files, and input data files in 'input'.

Typing

```
> python stm.py
```

will provide you with a help. Mandatory options are input wind and temperture fields, sensible options are to provide also names for the output files! Try:

```
> python stm.py -w input/wind_199801.m -T input/temp_199801.m
```

Analysis of output

We provide a convenient tool to view the data that should work on linux and windows, but probably not on Mac. To start the viewer, simply type

```
> python stmview.py -w windfile -T tempfile
```

Figure **??** shows two screenshots.

Further, there are some simple IDL programs that analyse the data. They are in the folder 'aux'; a simple program to plot the output is plot_overview: start IDL, and type

```
.r plot_overview, tra_fname, lcp_fname, plot_fname='test.ps'
```

where the first two files are the output files from stm.py; and the plot (postscript file) will have the name 'test.ps'.

The output from 'stm.py' are two very simple ascii-files that you can easily read with your favourite tool; you are encouraged to write your own, more sophisticated analysis tools (you are welcome to use the provided files as templates).

Finally, note that you have to organise the output yourself. We recommend making subdirectories for each type of experiment you do, and have all output and plot files in these directories.

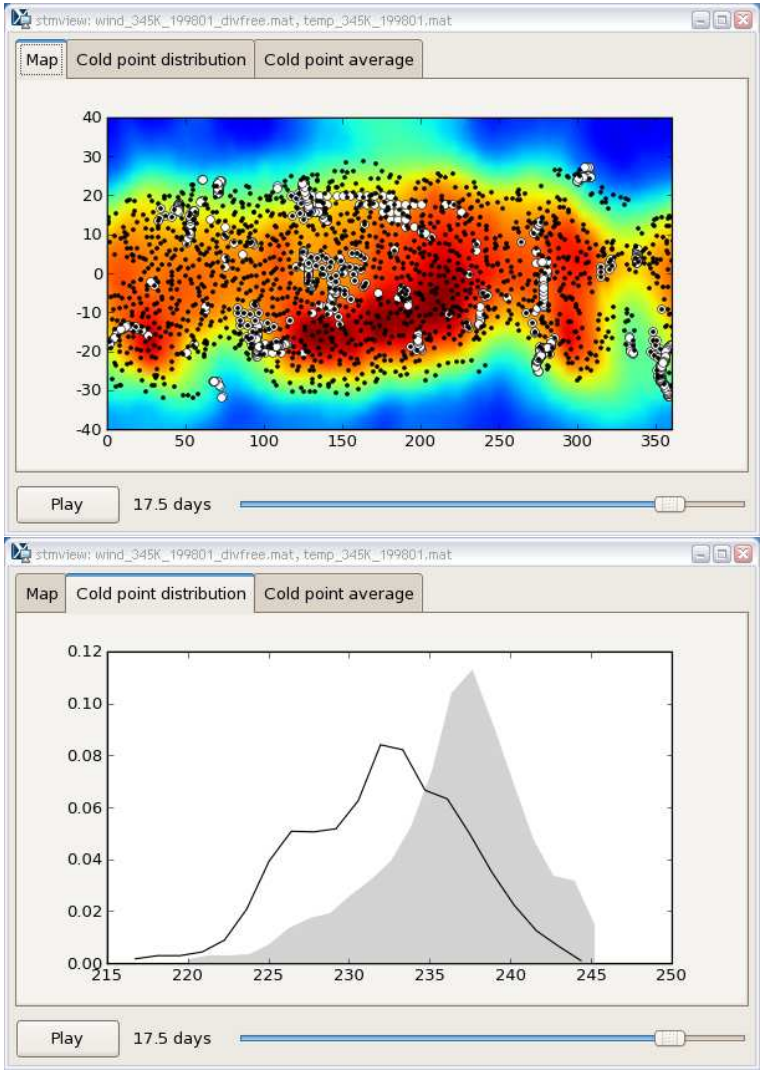

Figure 37: Sample screenshots from stmviewer.py.

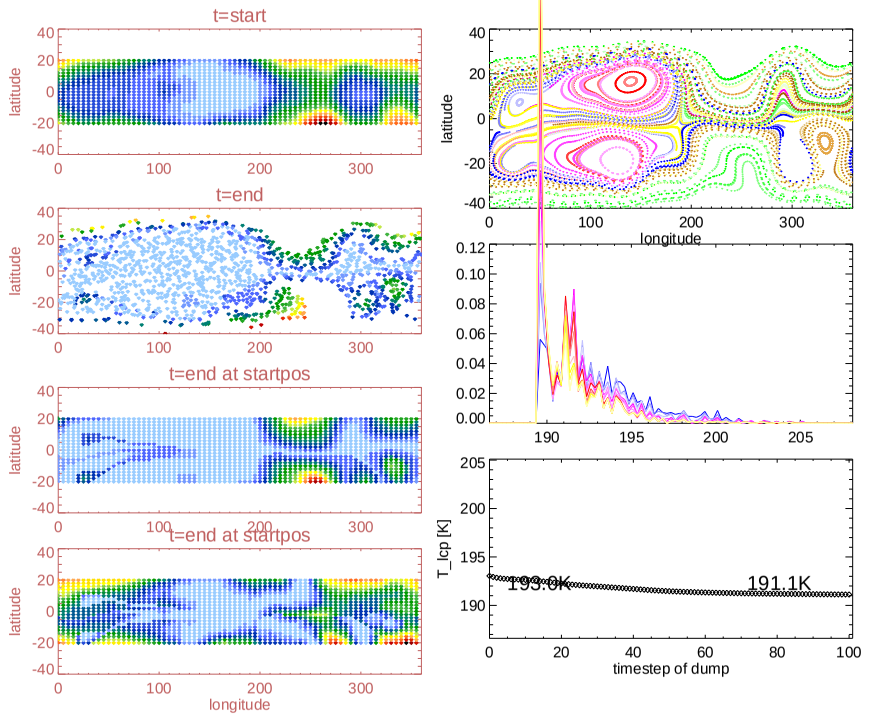

Figure 38: Sample output from stm.py plotted with plot_overview.pro. 380K_200101_divfree. (NOTE: Figure may be outdated.)

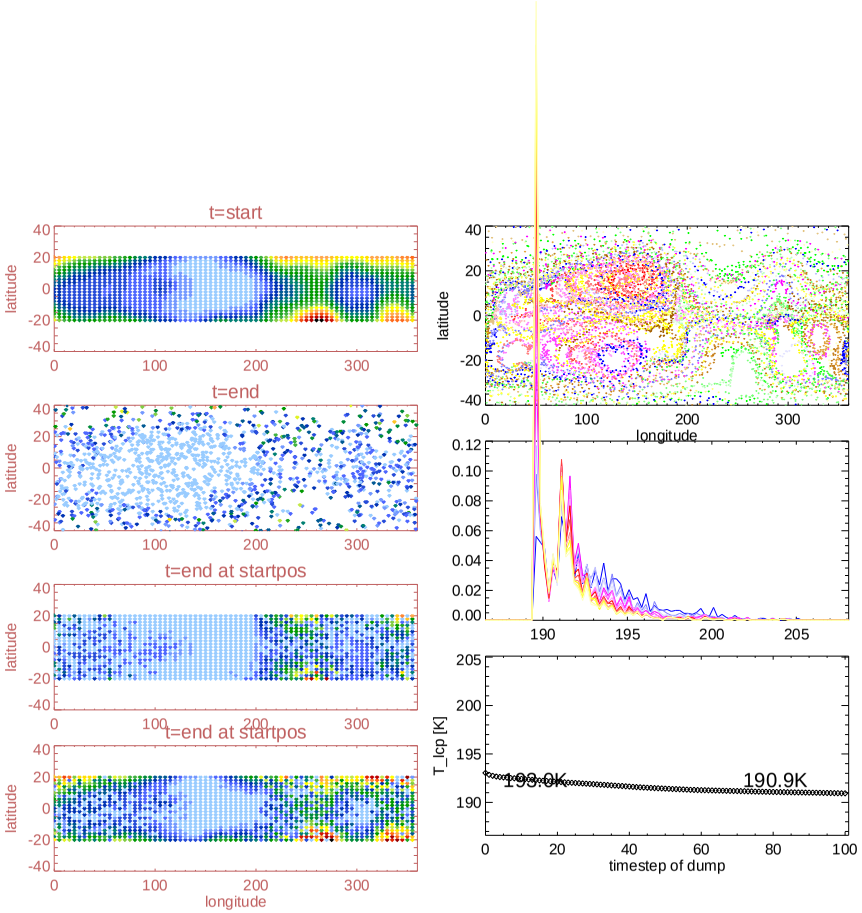

Figure 39: Sample output from stm.py plotted with plot_overview.pro. 380K_200101_divfree_D0001. (NOTE: Figure may be outdated.)

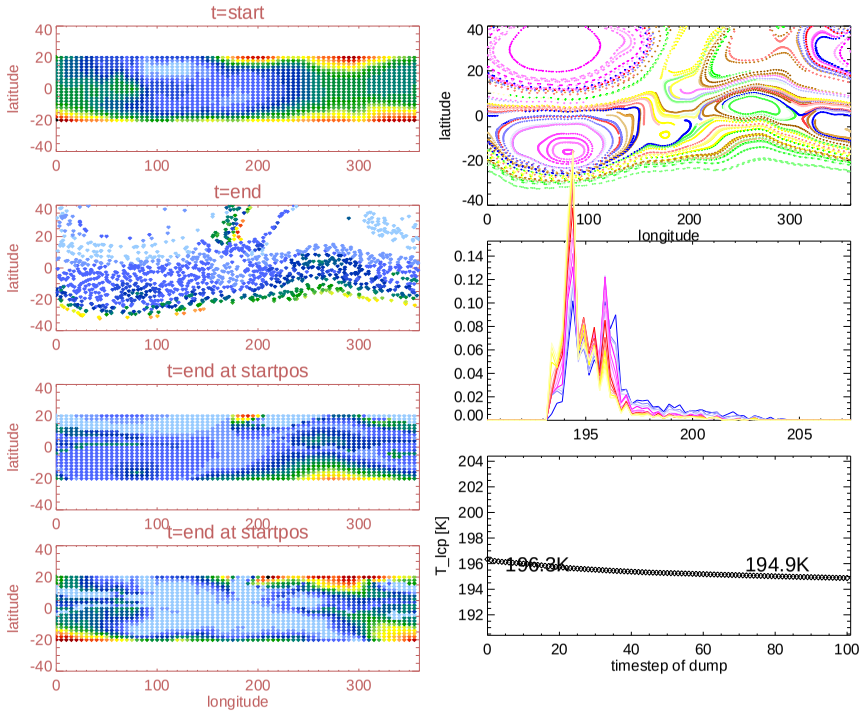

Figure 40: Sample output from stm.py plotted with plot_overview.pro. 380K_200107_divfree. (NOTE: Figure may be outdated.)

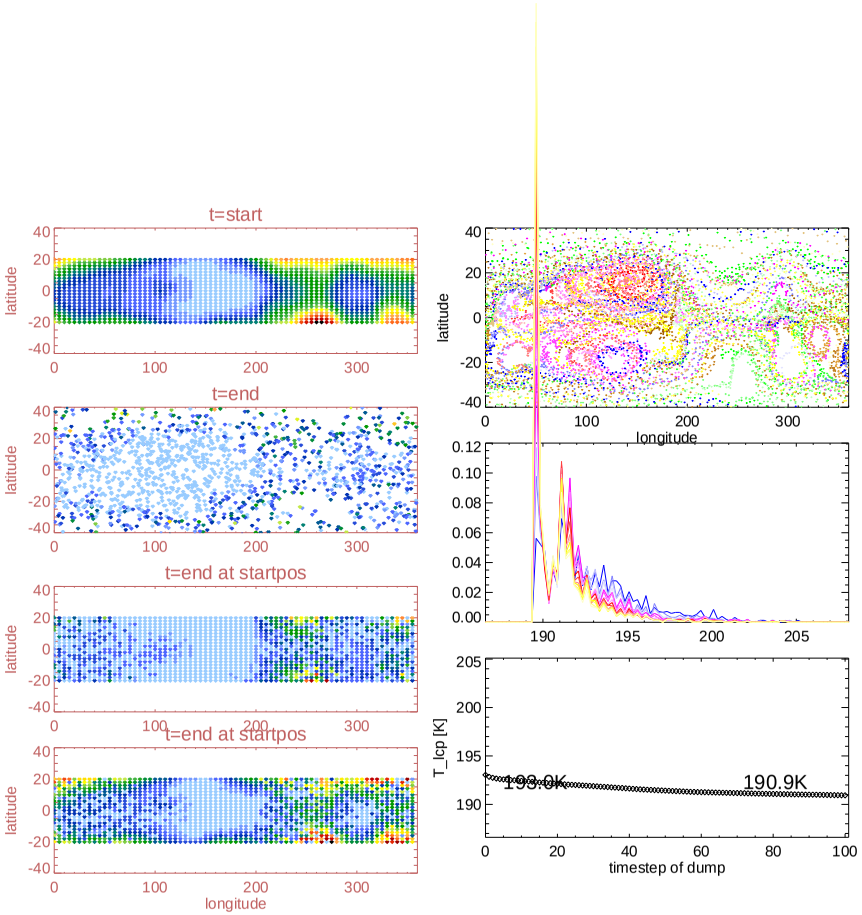

Figure 41: Sample output from stm.py plotted with plot_overview.pro. 380K_200101_divfree_D0001. (NOTE: Figure may be outdated.)

4.2 Experiment A: Divergence-free wind fields

(1) Run the model with input files 'divfree' for all conditions.

(2) What happens with increasing length of integration?

4.3 Experiment B: Original wind fields

Note: These wind fields are taken 'as is' and as such have divergence/convergence, which is accompanied with variations in vertical velocity - which we do ignore here. Hence, these calculations merely serve the purpose to illustrate what happens when air masses do not follow closed streamlines.

(1) Redo all previous calculations with the divergent wind fields.

(2) Compare the results to those of the non-divergent wind fields. What do you observe?

(3) What's the 'problem' with divergent wind fields with respect to estimates of water vapour (hint - think about mass fluxes).

4.4 Experiment C: Diffusion

(1) Run the model with a number of input files, and modify the diffusivity. This experiment is also particularly interesting for 'divergence free' input fields. What do you observe?

4.5 Experiment D: ENSO

(1) Analyse in detail the changes as a result of ENSO. (1998 versus 2001). What do you note?

(2) What happens if you remove the mean temperature difference between El-Nino and 'standard' year? (I.e. manipulate the input temperature fields.)

(3) Substitute flow/temperature fields between the cases (i.e. take 199801 wind with 200101 temperature, and compare with 200101wind/temperature; and conversely). What do you observe?

(4) Can you explain differences std-El-Nino with 'linear' arguments? (Probably no - coupled terms v'T' etc are important.)

5 Bibliography

Baldwin M.P., *et al.* (2001), The quasi-biennial oscillation, *Rev. Geophys., 39 (2),* 179–229.

Fueglistaler, S., B.P. Luo, C. Voigt, et al. (2002), NAT-rock formation by mother clouds: a microphysical model study *Atmos. Chem. Phys., 2,* 93-98.

Fueglistaler, S., H. Wernli, T. Peter (2004), Tropical troposphere-to-stratosphere transport inferred from trajectory calculations, *J. Geophys. Res., 109*, D03108, doi:10.1029/2003JD004069.

Fueglistaler, S., M. Bonazzola, P.H. Haynes, T. Peter (2005), Stratospheric water vapor predicted from the Lagrangian temperature history of air entering the stratosphere in the tropics, *J. Geophys. Res., 110 (D8),* D08107, doi:10.1029/2004JD005516.

Fueglistaler, S., P.H. Haynes (2005), Control of interannual and longer-term variability of stratospheric water vapor, *J. Geophys. Res., 110 (D24),* D24108, doi:10.1029/2005JD006019.

Fueglistaler, S., A.E. Dessler, T.J. Dunkerton, I. Folkins, Q. Fu, P.W. Mote (2009), Tropical Tropopause Layer, *Rev. Geophys., 47,* RG1004.

Gill, A.E. (1980), Some simple solutions for heat induced tropical circulation, *Q.J.R. Meteorol. Soc., 106,* 447–462.

Holton, J.R., P.H. Haynes, M.E. McIntyre, A.R. Douglass, R.B. Rood, and L. Pfister (1995), Stratosphere-troposphere exchange, *Rev. Geophys., 33,* 403–440.

Kärcher, B., U. Lohmann, (2002), A parametrization of cirrus cloud formation: Homogeneous freezing of supercooled aerosols, *J. Geophys. Res., 107*, 4010, doi:10.1029/2001JD000470.

Koop, T., B.P. Luo, A. Tsias, and Th. Peter, (2000), Water activity as the determinant for homogeneous ice nucleation in aqueous solutions, Nature, 406, 611–614, 2000.

Mullin, J.W., (2001), Crystalization, *Butterworth-Heinemann, 4th. ed.,* Oxford.

Murphy, D.M., T. Koop (2005), Review of the vapour pressures of ice and supercooled water for atmospheric applications, *Q. J. Roy. Meteorol. Soc., 131,* 1539–1565.

Pruppacher H.R., and J. D Klett, (1997), Microphysics of Clouds and Precipitation, *Kluwer Academic Publishers, 2nd ed.*

Weinstock, E.M., E.J. Hintsa, A.E. Dessler, J.G. Anderson (1995), Measurements of water vapor in the tropical lower stratosphere during the CEPEX campaign: results and interpretation, *Geophys. Res. Letts., 22,* 3231–3234.